

Study of quasi-two-body $B^0 \rightarrow T(\pi\pi, K\bar{K}, \pi\eta)$ decays in perturbative QCD approach

Lun-Lian Mu^{1,*} and Xian-Qiao Yu^{1,†}

¹*School of Physical Science and Technology, Southwest University, Chongqing 400715, China*

(Dated: January 15, 2025)

In this study, we calculate the CP -averaged branching ratios and the direct CP -violating asymmetries of the three body decays $B^0 \rightarrow T(\pi\pi, K\bar{K}, \pi\eta)$ in the perturbative QCD approach, where T denotes tensor mesons $a_2(1320)$, $K_2^*(1430)$, $f_2(1270)$ and $f_2'(1525)$, and the daughter branching is $f_0(980) \rightarrow \pi\pi$, $K\bar{K}$, $f_0(500) \rightarrow \pi\pi$, $a_0(980) \rightarrow K\bar{K}$, $\pi\eta$. By introducing two-meson distribution amplitudes parametrized by the timelike form factors, the three-body decay is simplified to quasi-two-body decay. The scalar mesons $a_0(980)$, $f_0(980)$ and $f_0(500)$ are regarded as the lowest-lying $q\bar{q}$ state, considering the effect of mixing angle θ between $f_0(980)$ and $f_0(500)$, ϕ between $f_2(1270)$ and $f_2'(1525)$ on our calculations. We found the following (a) With $\theta = 135^\circ$, we evaluate the branching fractions of $B^0 \rightarrow K_2^*(1430)f_0(980) \rightarrow \pi^+\pi^-\pi^-$ to be 4.30×10^{-6} , then under the narrow-width approximation we extract the branching fraction of the decay $B^0 \rightarrow K_2^*(1430)f_0(980)$ to be 8.78×10^{-6} , which is consistent with the current experimental data well. (b) The decay rates for the considered decay modes are generally in the order of 10^{-8} to 10^{-5} . (c) The branching fractions are sensitive to the θ , and the opposite is true for ϕ . The ϕ is really small, so the decay branching ratio has only little change, except for some decays involving $f_2'(1525)$. (d) The θ and ϕ can bring remarkable change to the direct CP asymmetries of pure penguin processes so that it is not 0. (e) We calculate the relative partial decay widths $\Gamma(a_0 \rightarrow K\bar{K})/\Gamma(a_0 \rightarrow \pi\eta)$ and the ratio $\mathcal{B}(f_0 \rightarrow K^+K^-)/\mathcal{B}(f_0 \rightarrow \pi^+\pi^-)$, which are in agreement with the existing experimental values. Our results can help one to understand the internal structure of scalar mesons and the nature of tensor mesons and can be tested by future experiments.

I. INTRODUCTION

Three-body hadronic B meson decays can be important for testing the Standard Model (SM) by measuring the associated Cabibbo-Kobayashi Maskawa (CKM) matrix parameters such as the weak phases α , β , and γ , understanding the potential mechanisms of hadronic weak decays and CP violation, and discovering new physics[1]. From the point of view of the spin-parity quantum numbers J^P , $J^P = 2^+, 1^+, 0^+, 0^-$ represents tensor mesons (T), vector mesons (V), scalar mesons (S) and pseudoscalar mesons (P), respectively[2]. In this paper we study the tensors including isovector mesons $a_2(1320)$, isodoublet states $K_2^*(1430)$ and two isosinglet mesons $f_2(1270)$, $f_2'(1525)$ [3, 4]. The factorizable amplitude with a tensor meson emitted is prohibited because a tensor meson cannot be created from the $(V \pm A)$ or $(S \pm P)$ currents[2]. The isoscalar tensor states $f_2(1270)$ and $f_2'(1525)$ have a mixing. From the experiment that $f_2(1270)$ decays dominantly into $\pi\pi$, and KK is the dominant decay mode of $f_2'(1525)$, we can know that the $f_2(1270) - f_2'(1525)$ mixing angle ϕ is really small, $f_2(1270)$ is nearly $(u\bar{u} + d\bar{d})/\sqrt{2}$, and $f_2'(1525)$ is mainly $s\bar{s}$ [4–6]. The physical states $f_2(1270)$ and $f_2'(1525)$ can be given by[2]

$$\begin{aligned} f_2(1270) &= f_2^n \cos \phi + f_2^s \sin \phi, \\ f_2'(1525) &= f_2^n \sin \phi - f_2^s \cos \phi, \end{aligned} \quad (1)$$

we use the quark-flavor basis, with $f_2^n = \frac{1}{\sqrt{2}}(u\bar{u} + d\bar{d})$, $f_2^s = s\bar{s}$. Moreover, it is also theoretically found that the mixing angle $\phi = 5.8^\circ$ [5], 7.8° [6], $(9 \pm 1)^\circ$ [7]. In two-body decays, there have been experimental and theoretical studies of $B \rightarrow PT, VT, ST, TT$ [8–11]. In three-body decays, much work has been done on the tensor as a resonance state[12–16]. For the first time, we treat the tensor as a nonresonant state, which is necessary to gain insight into the relevant decays and facilitates the exploration of the nature of the scalar resonances involved.

The identification of scalar resonances is a long-standing challenge. Scalar resonances are difficult to deal with because some of them have very broad decay widths, leading to strong overlap between the resonance and the background. In addition, the fundamental structure of scalar mesons is still quite controversial on the theoretical side. Currently, there are two main different scenarios, the so-called Scenario I (S-I) and Scenario II (S-II), to explain scalar mesons[17, 18]. In S-I, the mesons below or close to 1 GeV are considered as the lowest $q\bar{q}$ bound states, while mesons above 1 GeV are the first excited two-quark states. In contrast, in S-II, mesons near 1.5 GeV are regarded as ground two-quark states, while lighter mesons are identified with

* Electronic address: ml12631977415@163.com

† Electronic address: yuxq@swu.edu.cn

the dominant $q\bar{q}q\bar{q}$ state and possibly mixed with glueball states. Each scenario has its own physical meaning. In order to give quantitative predictions, we will only work in the S-I where $f_0(980)$ is regarded as the conventional two-quark $q\bar{q}$ state. The reason is that the $f_0(980)$ described by the four-quark state in S-II is too complex. It cannot be studied by factorization approaches[1]. In addition, the presence of nonstrange and strange quark contents in $f_0(980)$ and $f_0(500)$ has been confirmed by the experimental measurements of the decays $D_s^+ \rightarrow f_0\pi$, $\phi \rightarrow f_0\gamma$, $J/\psi \rightarrow f_0\omega$, $J/\psi \rightarrow f_0\phi$. $f_0(980)$ and $f_0(500)$ can be regarded as a mixture of $s\bar{s}$ and $(u\bar{u} + d\bar{d})/\sqrt{2}$ [19]. The mixing relation for the $f_0 - \sigma$ system[20],

$$\begin{pmatrix} \sigma \\ f_0 \end{pmatrix} = \begin{pmatrix} \cos \theta & -\sin \theta \\ \sin \theta & \cos \theta \end{pmatrix} \begin{pmatrix} f_n \\ f_s \end{pmatrix} \quad (2)$$

with $f_n = \frac{1}{\sqrt{2}}(u\bar{u} + d\bar{d})$, $f_s = s\bar{s}$. The mixing angle θ has not been determined experimentally or theoretically. The authors use the ratio between $J/\psi \rightarrow f_0\omega$ and $J/\psi \rightarrow f_0\phi$ to derive a mixing angle of $(34 \pm 6)^\circ$ and $(146 \pm 6)^\circ$ [21, 22]. The WA102 experiment on $f_0(980)$ production in central pp collisions yields a result of $\theta = (42.3^{+8.3}_{-5.5})^\circ$ and $(158 \pm 2)^\circ$ [23]. Furthermore, a phenomenological analysis of the radiative decays $\phi \rightarrow f_0\gamma$ and $f_0(980) \rightarrow \gamma\gamma$ shows that the $\theta = (138 \pm 6)^\circ$ is preferable[22]. Conservatively, we set θ to be a free parameter in this work.

It is well known that the multibody decay of heavy mesons involves more complex dynamics than the two-body decay and is difficult to describe in full phase space. It has been proposed that the factorization theorem for three-body B decay is approximately valid when two particles move collinear and the bachelor particle recoils back, which provides a theoretical framework for the study of resonance contributions based on the quasi-two-body decay mechanism. Three-body B decays have been extensively studied using various methods, such as those based on the symmetry principles[24], the QCD factorization approach[25–28], the perturbative QCD approach (pQCD)[29–32] and so on. Previous studies have shown that the multibody B meson decay branching ratio calculated by the pQCD approach based on the k_T factorization fits well with experimental results, which further verifies the effectiveness of this method[33–37]. In the pQCD approach, the three-body decay is simplified to the quasi-two-body decay and the pair of final state mesons is described by introducing the two-meson distribution amplitudes[38]. The contribution from the direct evaluation of hard b-quark decay kernels containing two virtual gluons is generally power suppressed, and the dominant contribution comes from the region where the two energetic light mesons are almost collimating to each other with an invariant mass below $O(\Lambda M_B)$, ($\Lambda = M_B - m_b$ is the difference in mass between the B meson and b quark). Then, the pQCD factorization formula for the three-body decay amplitude of the B meson is written as[39, 40]

$$\mathcal{A} = \mathcal{H} \otimes \phi_B \otimes \phi_{h_3} \otimes \phi_{h_1 h_2}, \quad (3)$$

where the hard decay kernel \mathcal{H} can be calculated by using the perturbative theory. The nonperturbative inputs ϕ_B , $\phi_{h_1 h_2}$ and ϕ_{h_3} are the distribution amplitudes of the B meson, $h_1 h_2$ pair and h_3 meson respectively.

In the last decades, several B decays with resonance states $a_0(980)$, $f_0(980)$ and $f_0(500)$ have been observed experimentally[41–43], and the corresponding theoretical calculations have attracted increasing attention. For example, the LHCb Collaboration and the Belle Collaboration have observed $B^0 \rightarrow J/\psi K^+ K^-$ decay and $B^\pm \rightarrow K^\pm f_0(980) \rightarrow K^\pm \pi^\mp \pi^\pm$ decay with $a_0(980)$, $f_0(980)$ as resonance states, respectively[44, 45]. In Ref.[46], the branching ratios of the $B \rightarrow J/\psi(K\bar{K}, \pi\eta)$ decays have been calculated with the resonances $a_0(980)$ and $a_0(1450)$, and the timelike form factors in the dimeson distribution amplitudes timelike form factors are parametrized by the Flatté model and the Breit-Wigner formula, respectively. The authors of Ref.[47], employing $a_0(980)$, $a_0(1450)$ and $a_0(1950)$ as resonances, studied the multiparticle configurations of isovector scalar mesons, in the $B \rightarrow a_0(\rightarrow K\bar{K}, \pi\eta)h$ by considering the width effects. In Ref.[48], the Breit-Wigner formula and the Bugg's model for $f_0(500)$ resonance, and the Flatté model for $f_0(980)$ resonance are adopted to study the quasi-two-body $B_{(s)}^0 \rightarrow \eta_c(2S)\pi^+\pi^-$. In Ref.[49], the author studied the quasi-two-body decays $B \rightarrow P f_0(500) \rightarrow P\pi^+\pi^-$. Based on the decay $B_s^0 \rightarrow SS(a_0(980), f_0(980), f_0(500))$ [37], the author predicted the branching ratios of the quasi-two-body decays $B_s^0 \rightarrow S[\rightarrow P_1 P_2]S$ [50]. In Ref.[51] and Ref.[52], the branching ratios of the $B \rightarrow K(\mathcal{R} \rightarrow K^+ K^-)$ and $B_{(s)} \rightarrow V\pi\pi$ decays with $f_0(980)$ resonance have been studied by considering the mixing of $s\bar{s}$ and $(u\bar{u} + d\bar{d})/\sqrt{2}$. Combining the theoretical results[10] and the BABAR Collaboration measurements of $B^0 \rightarrow K_2^*(1430)f_0(980)$ [53], we shall extend the study to $B^0 \rightarrow TS[\rightarrow P_1 P_2]$, where T denotes the tensor mesons $a_2(1320)$, $K_2^*(1430)$, $f_2(1270)$ and $f_2'(1525)$, and $P_1 P_2 = \pi\eta, \pi\pi, K\bar{K}$ is the final state meson pair.¹ For the mesons $f_0(980)$ and $f_0(500)$, $f_2(1270)$ and $f_2'(1525)$ we also adopt the corresponding mixing mechanism. The results presented in this paper can be validated in the LHCb and Belle II experiments in the near future.

This paper is organized as follows. In Sec II, we introduce the theoretical framework. Section III will give the numerical values and some discussion. Section IV contains our conclusions. The Appendix collects the explicit PQCD factorization formulas for all the decay amplitudes.

¹ a_0 , f_0 , and σ refer to $a_0(980)$, $f_0(980)$, and $f_0(500)$ respectively in the following text. Moreover a_2 , f_2 , and f_2' refer to $a_2(1320)$, $f_2(1270)$, and $f_2'(1525)$ respectively

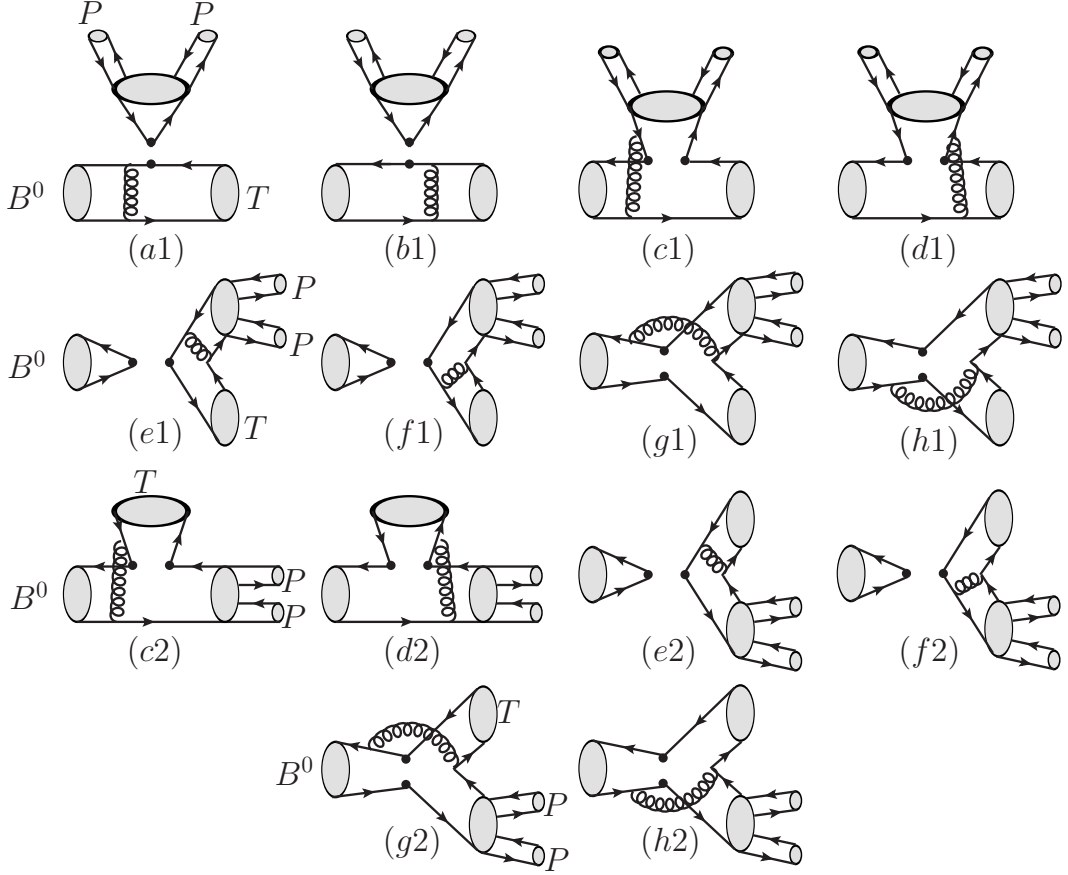


FIG. 1. The Feynman diagrams for the $B^0 \rightarrow TS[\rightarrow P_1 P_2]$ decays in pQCD. The symbol Black dot stands for the weak vertex, T means the tensor mesons, and $P_1 P_2$ denotes the final state meson pair; the corresponding relationship are $a_0(\pi\eta, K\bar{K})$, $f_0(\pi\pi, K\bar{K})$ and $\sigma(\pi\pi)$.

II. THE THEORETICAL FRAMEWORK AND HELICITY AMPLITUDES

A. The wave functions

The relevant weak effective Hamiltonian of the quasi-two-body $B^0 \rightarrow TS[\rightarrow P_1 P_2]$ decays can be written as[54]

$$\mathcal{H}_{eff} = \frac{G_F}{\sqrt{2}} \{ V_{ub}^* V_{uq} [C_1(\mu) O_1(\mu) + C_2(\mu) O_2(\mu)] - V_{tb}^* V_{tq} [\sum_{i=3}^{10} C_i(\mu) O_i(\mu)] \}, \quad (4)$$

where the $V_{ub}^* V_{uq}$ and CKM matrix elements with $q = d, s$ quark, the Fermi constant $G_F = 1.66378 \times 10^{-5} \text{GeV}^{-2}$, and C_i is the corresponding Wilson coefficient. The local four-quark operator $O_i(\mu)$ can be divided into the following three categories and the relevant Feynman diagrams illustrated in Fig. 1.

- Current-current (tree) operators:

$$O_1 = (\bar{b}_\alpha u_\beta)_{V-A} (\bar{u}_\beta q_\alpha)_{V-A}, O_2 = (\bar{b}_\alpha u_\alpha)_{V-A} (\bar{u}_\beta q_\beta)_{V-A}, \quad (5)$$

- QCD penguin operators:

$$\begin{aligned} O_3 &= (\bar{b}_\alpha q_\alpha)_{V-A} \sum_{q'} (\bar{q}'_\beta q'_\beta)_{V-A}, O_4 = (\bar{b}_\alpha q_\beta)_{V-A} \sum_{q'} (\bar{q}'_\beta q'_\alpha)_{V-A}, \\ O_5 &= (\bar{b}_\alpha q_\alpha)_{V-A} \sum_{q'} (\bar{q}'_\beta q'_\beta)_{V+A}, O_6 = (\bar{b}_\alpha q_\beta)_{V-A} \sum_{q'} (\bar{q}'_\beta q'_\alpha)_{V+A}, \end{aligned} \quad (6)$$

- Electroweak penguin operators:

$$\begin{aligned} O_7 &= \frac{3}{2} (\bar{b}_\alpha q_\alpha)_{V-A} \sum_{q'} e_{q'} (\bar{q}'_\beta q'_\beta)_{V+A}, O_8 = \frac{3}{2} (\bar{b}_\alpha q_\beta)_{V-A} \sum_{q'} e_{q'} (\bar{q}'_\beta q'_\alpha)_{V+A}, \\ O_9 &= \frac{3}{2} (\bar{b}_\alpha q_\alpha)_{V-A} \sum_{q'} e_{q'} (\bar{q}'_\beta q'_\beta)_{V-A}, O_{10} = \frac{3}{2} (\bar{b}_\alpha q_\beta)_{V-A} \sum_{q'} e_{q'} (\bar{q}'_\beta q'_\alpha)_{V-A}, \end{aligned} \quad (7)$$

where the subscripts α and β are the color indices and q' are the active quarks at the scale m_b , i.e. $q' = (u, d, s, c, b)$. The left-handed current is defined as $(\bar{b}_\alpha q_\alpha)_{V-A} = \bar{b}_\alpha \gamma_\mu (1 - \gamma_5) q_\alpha$, and the right-handed current is defined as $(\bar{q}'_\beta q'_\alpha)_{V+A} = \bar{q}'_\beta \gamma_\mu (1 + \gamma_5) q'_\alpha$.

In the light cone coordinates, we let the B^0 meson stay at rest, and choose the $P_1 P_2$ meson pair, and the final-state T move along the direction of $n = (1, 0, 0_T)$ and $v = (0, 1, 0_T)$, respectively. Thus, the momentum p_B of the B^0 meson, the total momentum $p = p_1 + p_2$ of the $P_1 P_2$ meson pair, and the momentum p_3 of the final state T are respectively

$$\begin{aligned} p_B &= \frac{M_B}{\sqrt{2}} (1, 1, 0_T), \\ p &= \frac{M_B}{\sqrt{2}} (1 - r^2, \eta, 0_T), \\ p_3 &= \frac{M_B}{\sqrt{2}} (r^2, 1 - \eta, 0_T), \end{aligned} \quad (8)$$

where M_B represents the mass of B^0 , $r = \frac{m_T}{M_B}$ is the mass ratio, and m_T refers to the mass of the final-state T . We think the variable $\eta = \omega^2 / (M_B^2 - m_T^2)$, and ω is the invariant mass of the $P_1 P_2$ meson pair, which satisfies the relation $\omega^2 = p^2$. Meanwhile, we define $\zeta = p_1^+ / p^+$ as one of the $P_1 P_2$ meson pair's momentum fractions. Accordingly, the kinematic variables of other components in the meson pair can be expressed as

$$\begin{aligned} p_1^- &= \frac{M_B}{\sqrt{2}} (1 - \zeta) \eta, \\ p_2^+ &= \frac{M_B}{\sqrt{2}} (1 - \zeta) (1 - r^2), \\ p_2^- &= \frac{M_B}{\sqrt{2}} \zeta \eta. \end{aligned} \quad (9)$$

We adopt x_B, z, x_3 to indicate the momentum fraction of the light quark in each meson with the range from zero to unity. So the light quark's momentum of the $B^0(k_B)$, $P_1 P_2(k)$ and $T(k_3)$ are defined as

$$\begin{aligned} k_B &= (0, \frac{M_B}{\sqrt{2}} x_B, k_{BT}), \\ k &= (\frac{M_B}{\sqrt{2}} z (1 - r^2), 0, k_T), \\ k_3 &= (\frac{M_B}{\sqrt{2}} r^2 x_3, \frac{M_B}{\sqrt{2}} (1 - \eta) x_3, k_{3T}). \end{aligned} \quad (10)$$

For the B^0 meson, the wave function can be expressed as[55–57]

$$\Phi_B = \frac{i}{\sqrt{2N_c}}(\not{p}_B + M_B)\gamma_5\phi_B(x_B, b_B), \quad (11)$$

where $N_c = 3$ is the color factor. The light cone distribution amplitude(LCDA) $\phi_B(x_B, b_B)$ is explicitly expressed as

$$\phi_B(x_B, b_B) = N_B x_B^2 (1 - x_B)^2 \exp\left[-\frac{M_B^2 x_B^2}{2\omega_b^2} - \frac{1}{2}(\omega_b b_B)^2\right], \quad (12)$$

where the N_B is the normalization constant, which can be determined by the normalization condition

$$\int_0^1 \phi_B(x_B, b_B = 0) dx = f_B / (2\sqrt{2N_c}), \quad (13)$$

with the decay constant $f_B = (0.19 \pm 0.02)\text{GeV}$. The corresponding shape parameter ω_b in the LCDA of the B^0 meson is usually taken as the value $(0.40 \pm 0.04)\text{GeV}$.

In the quark model, the tensor meson with $J^{PC} = 2^{++}$ has angular momentum $L = 1$ and spin $S = 1$. The polarization of $\lambda = \pm 2$ vanishes in the three-body decays $B^0 \rightarrow TS[\rightarrow P_1 P_2]$ because of angular momentum conservation. In this case, the wave function of the tensor meson is very similar to the vector meson and can be defined as[58, 59]

$$\begin{aligned} \Phi_T &= \frac{1}{\sqrt{2N_c}}[m_T \not{\epsilon}_{\bullet L}^* \phi_T(x) + \not{\epsilon}_{\bullet L}^* \not{P} \phi_T^t(x) + m_T^2 \frac{\epsilon_{\bullet} \cdot v}{P \cdot v} \phi_T^s(x)] \\ \Phi_T^\perp &= \frac{1}{\sqrt{2N_c}}[m_T \not{\epsilon}_{\bullet \perp}^* \phi_T^v(x) + \not{\epsilon}_{\bullet \perp}^* \not{P} \phi_T^T(x) + m_T i \epsilon_{\mu\nu\rho\sigma} \gamma_5 \gamma^\mu \epsilon_{\bullet \perp}^{\nu} n^\rho v^\sigma \phi_T^a(x)] \end{aligned} \quad (14)$$

with $\epsilon^{0123} = 1$. The reduced polarization vector $\epsilon_{\bullet\mu} = \frac{\epsilon_{\mu\nu} v^\nu}{P \cdot v}$, in which $\epsilon_{\mu\nu}$ is the polarization tensor of the tensor meson. The expressions of twist-2 and twist-3 LCDAs are given as

$$\begin{aligned} \phi_T(x) &= \frac{f_T}{2\sqrt{2N_c}} \phi_\parallel(x), \phi_T^t(x) = \frac{f_T^\perp}{2\sqrt{2N_c}} h_\parallel^t(x), \\ \phi_T^s(x) &= \frac{f_T^\perp}{4\sqrt{2N_c}} \frac{d}{dx} h_\parallel^s(x), \phi_T^T(x) = \frac{f_T^\perp}{2\sqrt{2N_c}} \phi_\perp(x), \\ \phi_T^v(x) &= \frac{f_T}{2\sqrt{2N_c}} g_\perp^v(x), \phi_T^a(x) = \frac{f_T}{8\sqrt{2N_c}} \frac{d}{dx} g_\perp^a(x). \end{aligned} \quad (15)$$

with the detailed

$$\begin{aligned} \phi_{\parallel, \perp}(x) &= 30x(1-x)(2x-1), g_\perp^v(x) = 5(2x-1)^3, \\ h_\parallel^t(x) &= \frac{15}{2}(2x-1)(1-6x+6x^2), \\ h_\parallel^s(x) &= 15x(1-x)(2x-1), g_\perp^a(x) = 20x(1-x)(2x-1). \end{aligned} \quad (16)$$

In this work, the S-wave two-meson DA is written in the form

$$\Phi_{P_1 P_2}^S = \frac{1}{\sqrt{2N_c}}[\not{p}\phi_S(z, \zeta, \omega^2) + \omega\phi_S^s(z, \zeta, \omega^2) + \omega(\not{n} \not{p} - 1)\phi_S^t(z, \zeta, \omega^2)], \quad (17)$$

and the asymptotic forms of the individual twist-2 and twist-3 DAs ϕ_S and $\phi_S^{s,t}$ are parametrized as

$$\begin{aligned} \phi_S(z, \zeta, \omega^2) &= \frac{9F_S(\omega)}{\sqrt{2N_c}} a_2 z(1-z)(1-2z), \\ \phi_S^s(z, \zeta, \omega^2) &= \frac{F_S(\omega)}{2\sqrt{2N_c}}, \\ \phi_S^t(z, \zeta, \omega^2) &= \frac{F_S(\omega)}{2\sqrt{2N_c}}(1-2z). \end{aligned} \quad (18)$$

with the Gegenbauer coefficient $a_2 = 0.3 \pm 0.1$ for a_0 and $a_2 = 0.3 \pm 0.2$ for f_0 [44, 52, 60]. $F_S(\omega)$ is the timelike form factor, which can factorize the strong interactions between the resonance and the final-state meson pair, as well as the elastic rescattering processes of the final-state meson pair.

For the scalar resonances a_0 and f_0 , we adopt the Flatté parametrization where the resulting line shape is above and below the threshold of the intermediate particle. The pole masses of the a_0 and f_0 resonances are both close to the $K\bar{K}$ threshold, and the main decay channels are $a_0 \rightarrow \pi\eta, K\bar{K}$ and $f_0 \rightarrow \pi\pi, K\bar{K}$. Since the Flatté parametrization shows a scaling invariance and does not allow for an extraction of individual partial decay widths when the coupling of a resonance to the channel opening nearby is very strong, we employ the modified Flatté model

$$F_S^{f_0}(\omega) = \frac{m_{f_0}^2}{m_{f_0}^2 - \omega^2 - im_{f_0}(g_{\pi\pi}\rho_{\pi\pi} + g_{KK}\rho_{KK}F_{KK}^2)}, \quad (19)$$

for the f_0 resonance[31, 52] and

$$F_S^{a_0}(\omega) = \frac{C_{a_0}m_{a_0}^2}{m_{a_0}^2 - \omega^2 - i(g_{\pi\eta}^2\rho_{\pi\eta} + g_{KK}^2\rho_{KK})}, \quad (20)$$

for the a_0 resonance[46]. The timelike form factor of the resonant state a_0 is parametrized by the complex amplitude $C_{a_0} = |C_{a_0}|e^{i\phi_{a_0}}$, where the value depends on whether the final state mesons are $\pi\eta$ or $K\bar{K}$. For the $a_0 \rightarrow K\bar{K}$ channel, the magnitude of the complex amplitude $|C_{a_0}^{KK}| = 1.07$ and the phase angle $\phi_{a_0} = 82^\circ$. When the channel is $a_0 \rightarrow \pi\eta$, the phase angle remains the same as in the $K\bar{K}$ system, and the amplitude magnitude satisfies $C_{a_0}^{\pi\eta}/C_{a_0}^{KK} = g_{a_0\pi\eta}/g_{a_0KK}$. The definition of the strong coupling constants $g_{a_0KK}(g_{a_0\pi\eta})$ can be found in the literature[47, 61]. We determined the strong coupling constants g_{a_0KK} and $g_{a_0\pi\eta}$ by using the relation $g_{a_0KK}(g_{a_0\pi\eta})/(4\sqrt{\pi}) = g_{KK}(g_{\pi\eta})$ and the coupling constants $g_{\pi\eta} = 0.324$ GeV, $g_{KK}^2/g_{\pi\eta}^2 = 1.03$ from the Crystal Barrel experiment. Meanwhile, we employ the coupling constants $g_{\pi\pi} = 0.165 \pm 0.018$ GeV and $g_{KK}/g_{\pi\pi} = 4.21 \pm 0.33$ for f_0 [52, 62], and introduce the factor $F_{KK} = e^{-\alpha q^2}$ into the timelike form factor $F_S^{f_0}(\omega)$ to suppress the $K\bar{K}$ contribution with the parameter $\alpha = 2.0 \pm 1.0$ GeV⁻². In addition, the ρ factors are chosen as:

$$\rho_{\pi\eta} = \sqrt{[1 - (\frac{m_\eta - m_\pi}{\omega})^2][1 - (\frac{m_\eta + m_\pi}{\omega})^2]}, \quad (21)$$

$$\rho_{\pi\pi} = \frac{2}{3}\sqrt{1 - \frac{4m_{\pi^\pm}^2}{\omega^2}} + \frac{1}{3}\sqrt{1 - \frac{4m_{\pi^0}^2}{\omega^2}}, \quad (22)$$

$$\rho_{KK} = \frac{1}{2}\sqrt{1 - \frac{4m_{K^\pm}^2}{\omega^2}} + \frac{1}{2}\sqrt{1 - \frac{4m_{K^0}^2}{\omega^2}}. \quad (23)$$

Following the analysis of the LHCb Collaboration[63–65], and motivated by the studies in Refs[36, 48, 50, 66, 67], the shape of the σ resonance can be well described by the Breit-Wigner model:

$$F_S^\sigma(\omega) = \frac{C_\sigma m_\sigma^2}{m_\sigma^2 - \omega^2 - im_\sigma\Gamma(\omega)}, \quad (24)$$

with the factor $C_\sigma = 3.50$. The energy-dependent width $\Gamma(\omega)$ in the case of a scalar resonance decaying into pion pair can be parametrized as

$$\Gamma(\omega) = \Gamma_0 \frac{m_\sigma}{\omega} \left(\frac{\omega^2 - 4m_\pi^2}{m_\sigma^2 - 4m_\pi^2} \right)^{\frac{1}{2}}, \quad (25)$$

where $\Gamma_0 = 0.40$ GeV is the width of the resonance.

B. Helicity amplitudes

According to the typical Feynman diagrams as shown in Fig. 1, the total decay amplitude for each considered decay mode in this work is given as follows:

$$\begin{aligned}
 \mathcal{A}(B^0 \rightarrow K_2^* f_s [\rightarrow \pi^+ \pi^-, K^+ K^-]) = & -\frac{G_F}{\sqrt{2}} V_{tb}^* V_{ts} \left[\left(\frac{1}{3} C_5 - \frac{1}{6} C_7 + C_6 - \frac{1}{2} C_8 \right) (F_S^{SP} + A_S^{SP}) \right. \\
 & + \left(\frac{1}{3} C_3 - \frac{1}{6} C_9 + C_4 - \frac{1}{2} C_{10} \right) A_S^{LL} + (C_6 - \frac{1}{2} C_8) M_S^{SP} \\
 & + (C_3 - \frac{1}{2} C_9 + C_4 - \frac{1}{2} C_{10}) M_S^{LL} + (C_3 - \frac{1}{2} C_9) W_S^{LL} \\
 & \left. + (C_5 - \frac{1}{2} C_7) (M_S^{LR} + W_S^{LR}) \right], \tag{26}
 \end{aligned}$$

$$\begin{aligned}
 \mathcal{A}(B^0 \rightarrow K_2^* f_n [\rightarrow \pi^+ \pi^-, K^+ K^-]) = & \frac{G_F}{2} \{ V_{ub}^* V_{us} C_2 M_S^{LL} - V_{tb}^* V_{ts} [(C_4 + \frac{1}{3} C_3 - \frac{1}{2} C_{10} - \frac{1}{6} C_9) A_T^{LL} \\
 & + (C_6 + \frac{1}{3} C_5 - \frac{1}{2} C_8 - \frac{1}{6} C_7) A_T^{SP} + (C_3 - \frac{1}{2} C_9) (M_T^{LL} + W_T^{LL}) \\
 & + (C_5 - \frac{1}{2} C_7) (M_T^{LR} + W_T^{LR}) + (2C_6 + \frac{1}{2} C_8) M_S^{SP} \\
 & + (2C_4 + \frac{1}{2} C_{10}) M_S^{LL}] \}, \tag{27}
 \end{aligned}$$

$$\begin{aligned}
 \mathcal{A}(B^0 \rightarrow K_2^* a_0^0 [\rightarrow \pi^0 \eta, K^+ K^-]) = & \frac{G_F}{2} \{ V_{ub}^* V_{us} C_2 M_S^{LL} - V_{tb}^* V_{ts} [(-C_4 - \frac{1}{3} C_3 + \frac{1}{2} C_{10} + \frac{1}{6} C_9) A_T^{LL} \\
 & + (-C_6 - \frac{1}{3} C_5 + \frac{1}{2} C_8 + \frac{1}{6} C_7) A_T^{SP} + (-C_3 + \frac{1}{2} C_9) (M_T^{LL} + W_T^{LL}) \\
 & + (-C_5 + \frac{1}{2} C_7) (M_T^{LR} + W_T^{LR}) + \frac{3}{2} C_8 M_S^{SP} + \frac{3}{2} C_{10} M_S^{LL}] \}, \tag{28}
 \end{aligned}$$

$$\begin{aligned}
 \mathcal{A}(B^0 \rightarrow K_2^{*+} a_0^- [\rightarrow \pi^- \eta, K^- \bar{K}^0]) = & \frac{G_F}{\sqrt{2}} \{ V_{ub}^* V_{us} C_1 M_T^{LL} - V_{tb}^* V_{ts} [(C_4 + \frac{1}{3} C_3 - \frac{1}{2} C_{10} - \frac{1}{6} C_9) A_T^{LL} \\
 & + (C_6 + \frac{1}{3} C_5 - \frac{1}{2} C_8 - \frac{1}{6} C_7) A_T^{SP} + (C_3 - \frac{1}{2} C_9) W_T^{LL} \\
 & + (C_5 - \frac{1}{2} C_7) W_T^{LR} + (C_3 + C_9) M_T^{LL} + (C_5 + C_7) M_T^{LR}] \}, \tag{29}
 \end{aligned}$$

$$\mathcal{A}(B^0 \rightarrow a_2^0 f_s [\rightarrow \pi^+ \pi^-, K^+ K^-]) = -\frac{G_F}{2} V_{tb}^* V_{td} \left[\left(\frac{1}{2} C_{10} - C_4 \right) M_S^{LL} + \left(\frac{1}{2} C_8 - C_6 \right) M_S^{SP} \right], \tag{30}$$

$$\begin{aligned}
 \mathcal{A}(B^0 \rightarrow a_2^0 f_n [\rightarrow \pi^+ \pi^-, K^+ K^-]) = & \frac{G_F}{2\sqrt{2}} \{ V_{ub}^* V_{ud} [(C_1 + \frac{1}{3} C_2) (A_S^{LL} + A_T^{LL}) \\
 & + C_2 (M_T^{LL} - M_S^{LL} + W_T^{LL} + W_S^{LL})] \\
 & - V_{tb}^* V_{td} [(-\frac{1}{3} C_3 + \frac{3}{2} C_7 + \frac{5}{3} C_9 - C_4 + \frac{1}{2} C_8 + C_{10}) (A_S^{LL} + A_T^{LL}) \\
 & + (\frac{1}{6} C_7 - \frac{1}{3} C_5 - C_6 + \frac{1}{2} C_8) (A_S^{SP} + A_T^{SP} + F_S^{SP}) \\
 & + (\frac{1}{2} C_9 + \frac{3}{2} C_{10} - C_3) (M_T^{LL} + W_T^{LL} + W_S^{LL}) - (2C_6 + \frac{1}{2} C_8) M_S^{SP} \\
 & + (\frac{1}{2} C_9 - \frac{1}{2} C_{10} - C_3 - 2C_4) M_S^{LL} + \frac{3}{2} C_8 (M_T^{SP} + W_T^{SP} + W_S^{SP}) \\
 & + (\frac{1}{2} C_7 - C_5) (M_T^{LR} + M_S^{LR} + W_T^{LR} + W_S^{LR})] \}, \tag{31}
 \end{aligned}$$

$$\begin{aligned}
\mathcal{A}(B^0 \rightarrow a_2^0 a_0^0 [\rightarrow \pi^0 \eta, K^+ K^-]) = & \frac{G_F}{2\sqrt{2}} \{ V_{ub}^* V_{ud} [(C_1 + \frac{1}{3}C_2)(A_S^{LL} + A_T^{LL}) + C_2(W_T^{LL} + W_S^{LL} - M_T^{LL} - M_S^{LL})] \\
& - V_{tb}^* V_{td} [-\frac{3}{2}C_8(M_T^{SP} + M_S^{SP}) + (C_3 - \frac{1}{2}C_9 - \frac{3}{2}C_{10})(M_T^{LL} + M_S^{LL})] \\
& + (\frac{7}{3}C_3 + \frac{1}{3}C_9 + \frac{5}{3}C_4 + \frac{2}{3}C_6 + \frac{1}{6}C_8 - \frac{1}{3}C_{10} + \frac{1}{2}C_7 + 2C_5)(A_S^{LL} + A_T^{LL}) \\
& + (C_3 - \frac{1}{2}C_9 + \frac{1}{2}C_{10} + 2C_4)(W_S^{LL} + W_T^{LL}) + (\frac{1}{2}C_8 + 2C_6)(W_S^{SP} + W_T^{SP}) \\
& + (\frac{1}{3}C_5 - \frac{1}{6}C_7 - \frac{1}{2}C_8 + C_6)(A_S^{SP} + A_T^{SP} + F_S^{SP}) \\
& + (C_5 - \frac{1}{2}C_7)(W_T^{LR} + W_S^{LR} + M_T^{LR} + M_S^{LR}) \}, \tag{32}
\end{aligned}$$

$$\begin{aligned}
\mathcal{A}(B^0 \rightarrow a_2^+ a_0^- [\rightarrow \pi^- \eta, K^- \bar{K}^0]) = & \frac{G_F}{\sqrt{2}} \{ V_{ub}^* V_{ud} [(C_1 + \frac{1}{3}C_2)A_S^{LL} + C_2W_S^{LL} + C_1M_T^{LL}] \\
& - V_{tb}^* V_{td} [(C_4 + C_{10})W_S^{LL} + (C_6 + C_8)W_S^{SP} \\
& + (C_3 + \frac{1}{3}C_4 + C_5 + \frac{1}{3}C_6 + C_7 + \frac{1}{3}C_8 + C_9 + \frac{1}{3}C_{10})A_S^{LL} \\
& + (C_3 + C_9)M_T^{LL} + (C_5 + C_7)M_T^{LR} + (C_5 - \frac{1}{2}C_7)W_T^{LR} \\
& + (\frac{4}{3}C_3 + \frac{4}{3}C_4 - \frac{2}{3}C_9 - \frac{2}{3}C_{10} + C_5 + \frac{1}{3}C_6 - \frac{1}{2}C_7 - \frac{1}{6}C_8)A_T^{LL} \\
& + (\frac{1}{3}C_5 + C_6 - \frac{1}{6}C_7 - \frac{1}{2}C_8)A_T^{SP} + (C_6 - \frac{1}{2}C_8)W_T^{SP} \\
& + (C_3 + C_4 - \frac{1}{2}C_9 - \frac{1}{2}C_{10})W_T^{LL}] \}, \tag{33}
\end{aligned}$$

$$\begin{aligned}
\mathcal{A}(B^0 \rightarrow a_2^- a_0^+ [\rightarrow \pi^+ \eta, K^+ \bar{K}^0]) = & \frac{G_F}{\sqrt{2}} \{ V_{ub}^* V_{ud} [(C_1 + \frac{1}{3}C_2)A_T^{LL} + C_2W_T^{LL} + C_1M_S^{LL}] \\
& - V_{tb}^* V_{td} [(C_4 + C_{10})W_T^{LL} + (C_6 + C_8)W_T^{SP} \\
& + (C_3 + \frac{1}{3}C_4 + C_5 + \frac{1}{3}C_6 + C_7 + \frac{1}{3}C_8 + C_9 + \frac{1}{3}C_{10})A_T^{LL} \\
& + (C_3 + C_9)M_S^{LL} + (C_5 + C_7)M_S^{LR} + (C_5 - \frac{1}{2}C_7)W_S^{LR} \\
& + (\frac{4}{3}C_3 + \frac{4}{3}C_4 - \frac{2}{3}C_9 - \frac{2}{3}C_{10} + C_5 + \frac{1}{3}C_6 - \frac{1}{2}C_7 - \frac{1}{6}C_8)A_S^{LL} \\
& + (\frac{1}{3}C_5 + C_6 - \frac{1}{6}C_7 - \frac{1}{2}C_8)A_S^{SP} + (C_6 - \frac{1}{2}C_8)W_S^{SP} \\
& + (C_3 + C_4 - \frac{1}{2}C_9 - \frac{1}{2}C_{10})W_S^{LL} + (C_6 + C_8 + \frac{1}{3}C_5 + \frac{1}{3}C_7)F_S^{SP}] \}, \tag{34}
\end{aligned}$$

$$\begin{aligned}
\mathcal{A}(B^0 \rightarrow f_2^s f_s [\rightarrow \pi^+ \pi^-, K^+ K^-]) = & -\frac{G_F}{\sqrt{2}} V_{tb}^* V_{td} [(C_3 + \frac{1}{3}C_4 + C_5 + \frac{1}{3}C_6 - \frac{1}{2}C_7 - \frac{1}{6}C_8 - \frac{1}{2}C_9 - \frac{1}{6}C_{10}) \\
& (A_T^{LL} + A_S^{LL}) + (C_4 - \frac{1}{2}C_{10})(W_S^{LL} + W_T^{LL}) \\
& + (C_6 - \frac{1}{2}C_8)(W_S^{SP} + W_T^{SP})], \tag{35}
\end{aligned}$$

$$\mathcal{A}(B^0 \rightarrow f_2^s f_n [\rightarrow \pi^+ \pi^-, K^+ K^-]) = -\frac{G_F}{2} V_{tb}^* V_{td} [(C_4 - \frac{1}{2}C_{10})M_T^{LL} + (C_6 - \frac{1}{2}C_8)M_T^{SP}], \tag{36}$$

$$\mathcal{A}(B^0 \rightarrow f_2^n f_s [\rightarrow \pi^+ \pi^-, K^+ K^-]) = -\frac{G_F}{2} V_{tb}^* V_{td} [(C_4 - \frac{1}{2}C_{10})M_S^{LL} + (C_6 - \frac{1}{2}C_8)M_T^{SP}], \tag{37}$$

$$\begin{aligned}
\mathcal{A}(B^0 \rightarrow f_2^n f_n [\rightarrow \pi^+ \pi^-, K^+ K^-]) = & \frac{G_F}{2\sqrt{2}} \{ V_{ub}^* V_{ud} [(C_1 + \frac{1}{3}C_2)(A_S^{LL} + A_T^{LL}) + C_2(M_T^{LL} + M_S^{LL} + W_T^{LL} + W_S^{LL})] \\
& - V_{tb}^* V_{td} [(\frac{7}{3}C_3 + 2C_5 + \frac{1}{2}C_7 + \frac{1}{3}C_9 + \frac{5}{3}C_4 - \frac{1}{3}C_{10} + \frac{2}{3}C_6 + \frac{1}{6}C_8)(A_S^{LL} + A_T^{LL}) \\
& + (\frac{1}{3}C_5 + C_6 - \frac{1}{6}C_7 - \frac{1}{2}C_8)(A_S^{SP} + A_T^{SP} + F_S^{SP}) \\
& + (C_3 + 2C_4 - \frac{1}{2}C_9 + \frac{1}{2}C_{10})(M_T^{LL} + M_S^{LL} + W_T^{LL} + W_S^{LL}) \\
& + (2C_6 + \frac{1}{2}C_8)(M_S^{SP} + M_T^{SP} + W_T^{SP} + W_S^{SP}) \\
& + (C_5 - \frac{1}{2}C_7)(M_T^{LR} + M_S^{LR} + W_T^{LR} + W_S^{LR})] \}, \tag{38}
\end{aligned}$$

$$\begin{aligned}
\mathcal{A}(B^0 \rightarrow f_2^n a_0^0 [\rightarrow \pi^0 \eta, K^+ K^-]) = & \frac{G_F}{2\sqrt{2}} \{ V_{ub}^* V_{ud} [(C_1 + \frac{1}{3}C_2)(A_S^{LL} + A_T^{LL}) + C_2(W_T^{LL} + W_S^{LL} - M_T^{LL} + M_S^{LL})] \\
& - V_{tb}^* V_{td} [\frac{3}{2}C_8(M_S^{SP} + W_T^{SP} + W_S^{SP}) + (\frac{1}{2}C_9 + \frac{3}{2}C_{10} - C_3)(M_S^{LL} + W_S^{LL} + W_T^{LL}) \\
& + (\frac{3}{2}C_7 - \frac{1}{3}C_3 + \frac{5}{3}C_9 - C_4 + \frac{1}{2}C_8 + C_{10})(A_S^{LL} + A_T^{LL}) \\
& + (\frac{1}{2}C_9 - C_3 - \frac{1}{2}C_{10} - 2C_4)M_T^{LL} - (\frac{1}{2}C_8 + 2C_6)M_T^{SP} \\
& + (\frac{1}{6}C_7 - \frac{1}{3}C_5 + \frac{1}{2}C_8 - C_6)(A_S^{SP} + A_T^{SP} + F_S^{SP}) \\
& + (\frac{1}{2}C_7 - C_5)(W_T^{LR} + W_S^{LR} + M_T^{LR} + M_S^{LR})] \}, \tag{39}
\end{aligned}$$

$$\mathcal{A}(B^0 \rightarrow f_2^s a_0^0 [\rightarrow \pi^0 \eta, K^+ K^-]) = -\frac{G_F}{2} V_{tb}^* V_{td} [(-C_4 + \frac{1}{2}C_{10})M_T^{LL} + (-C_6 + \frac{1}{2}C_8)M_T^{SP}], \tag{40}$$

where superscripts LL , LR , SP refer to the contributions from $(V - A) \otimes (V - A)$, $(V - A) \otimes (V + A)$ and $(S - P) \otimes (S + P)$ operators, respectively. The explicit formulas for the factorizable emission (annihilation) contributions F_S (A_S) shown in Fig. 1a1, b1, (e1, f1), and the nonfactorizable emission (annihilation) contributions M_S (W_S) from Fig. 1c1, d1, (g1, h1) can be obtained in Appendix, as A_T , M_T , W_T .

As discussed the quark flavor basis of the mixing, the decay amplitudes for the physical states are then

$$\mathcal{A}(B^0 \rightarrow K_2^* f_0 [\rightarrow \pi^+ \pi^-, K^+ K^-]) = \mathcal{A}(B^0 \rightarrow K_2^* f_n [\rightarrow \pi^+ \pi^-, K^+ K^-]) \sin \theta + \mathcal{A}(B^0 \rightarrow K_2^* f_s [\rightarrow \pi^+ \pi^-, K^+ K^-]) \cos \theta \tag{41}$$

$$\mathcal{A}(B^0 \rightarrow K_2^* \sigma [\rightarrow \pi^+ \pi^-]) = \mathcal{A}(B^0 \rightarrow K_2^* f_n [\rightarrow \pi^+ \pi^-]) \cos \theta - \mathcal{A}(B^0 \rightarrow K_2^* f_s [\rightarrow \pi^+ \pi^-]) \sin \theta \tag{42}$$

$$\mathcal{A}(B^0 \rightarrow f_2' a_0^0 [\rightarrow \pi^0 \eta, K^+ K^-]) = \mathcal{A}(B^0 \rightarrow f_2^n a_0^0 [\rightarrow \pi^0 \eta, K^+ K^-]) \sin \phi - \mathcal{A}(B^0 \rightarrow f_2^s a_0^0 [\rightarrow \pi^0 \eta, K^+ K^-]) \cos \phi \tag{43}$$

$$\mathcal{A}(B^0 \rightarrow f_2 a_0^0 [\rightarrow \pi^0 \eta, K^+ K^-]) = \mathcal{A}(B^0 \rightarrow f_2^n a_0^0 [\rightarrow \pi^0 \eta, K^+ K^-]) \cos \phi + \mathcal{A}(B^0 \rightarrow f_2^s a_0^0 [\rightarrow \pi^0 \eta, K^+ K^-]) \sin \phi \tag{44}$$

$$\begin{aligned}
\mathcal{A}(B^0 \rightarrow f_2' f_0 [\rightarrow \pi^+ \pi^-, K^+ K^-]) = & \mathcal{A}(B^0 \rightarrow f_2^n f_n [\rightarrow \pi^+ \pi^-, K^+ K^-]) \sin \phi \sin \theta \\
& + \mathcal{A}(B^0 \rightarrow f_2^n f_s [\rightarrow \pi^+ \pi^-, K^+ K^-]) \sin \phi \cos \theta \\
& - \mathcal{A}(B^0 \rightarrow f_2^s f_n [\rightarrow \pi^+ \pi^-, K^+ K^-]) \cos \phi \sin \theta \\
& - \mathcal{A}(B^0 \rightarrow f_2^s f_s [\rightarrow \pi^+ \pi^-, K^+ K^-]) \cos \phi \cos \theta \tag{45}
\end{aligned}$$

$$\begin{aligned}
\mathcal{A}(B^0 \rightarrow f_2 f_0 [\rightarrow \pi^+ \pi^-, K^+ K^-]) = & \mathcal{A}(B^0 \rightarrow f_2^n f_n [\rightarrow \pi^+ \pi^-, K^+ K^-]) \cos \phi \sin \theta \\
& + \mathcal{A}(B^0 \rightarrow f_2^n f_s [\rightarrow \pi^+ \pi^-, K^+ K^-]) \cos \phi \cos \theta \\
& + \mathcal{A}(B^0 \rightarrow f_2^s f_n [\rightarrow \pi^+ \pi^-, K^+ K^-]) \sin \phi \sin \theta \\
& + \mathcal{A}(B^0 \rightarrow f_2^s f_s [\rightarrow \pi^+ \pi^-, K^+ K^-]) \sin \phi \cos \theta
\end{aligned} \tag{46}$$

$$\begin{aligned}
\mathcal{A}(B^0 \rightarrow f_2' \sigma [\rightarrow \pi^+ \pi^-]) = & \mathcal{A}(B^0 \rightarrow f_2^n f_n [\rightarrow \pi^+ \pi^-]) \sin \phi \cos \theta - \mathcal{A}(B^0 \rightarrow f_2^n f_s [\rightarrow \pi^+ \pi^-]) \sin \phi \sin \theta \\
& - \mathcal{A}(B^0 \rightarrow f_2^s f_n [\rightarrow \pi^+ \pi^-]) \cos \phi \cos \theta + \mathcal{A}(B^0 \rightarrow f_2^s f_s [\rightarrow \pi^+ \pi^-]) \cos \phi \sin \theta
\end{aligned} \tag{47}$$

$$\begin{aligned}
\mathcal{A}(B^0 \rightarrow f_2 \sigma [\rightarrow \pi^+ \pi^-]) = & \mathcal{A}(B^0 \rightarrow f_2^n f_n [\rightarrow \pi^+ \pi^-]) \cos \phi \cos \theta - \mathcal{A}(B^0 \rightarrow f_2^n f_s [\rightarrow \pi^+ \pi^-]) \cos \phi \sin \theta \\
& + \mathcal{A}(B^0 \rightarrow f_2^s f_n [\rightarrow \pi^+ \pi^-]) \sin \phi \cos \theta - \mathcal{A}(B^0 \rightarrow f_2^s f_s [\rightarrow \pi^+ \pi^-]) \sin \phi \sin \theta
\end{aligned} \tag{48}$$

III. NUMERICAL RESULTS AND DISCUSSIONS

With the decay amplitudes \mathcal{A} , the differential branching ratio for the $B^0 \rightarrow TS[\rightarrow P_1 P_2]$ decays can be taken as

$$\frac{d\mathcal{B}}{d\omega} = \frac{\tau \omega |\vec{p}_1| |\vec{p}_3|}{32\pi^3 M_B^3} |\overline{\mathcal{A}}|^2, \tag{49}$$

where τ is the B meson lifetime, $|\vec{p}_1|$ and $|\vec{p}_3|$ respectively denote the magnitudes of momentum for one of the $P_1 P_2$ meson pairs and the tensor meson T

$$\begin{aligned}
|\vec{p}_1| &= \frac{\lambda^{1/2}(\omega^2, m_{P_1}^2, m_{P_2}^2)}{2\omega}, \\
|\vec{p}_3| &= \frac{\lambda^{1/2}(M_B^2, m_T^2, \omega^2)}{2\omega}
\end{aligned} \tag{50}$$

with the Källén function $\lambda(a, b, c) = a^2 + b^2 + c^2 - 2(ab + ac + bc)$.

Meanwhile, the direct CP asymmetries of these decays can be defined as

$$\mathcal{A}_{CP} = \frac{\mathcal{B}(\bar{B} \rightarrow \bar{f}) - \mathcal{B}(B \rightarrow f)}{\mathcal{B}(\bar{B} \rightarrow \bar{f}) + \mathcal{B}(B \rightarrow f)} \tag{51}$$

where \bar{f} is the CP conjugate state of f . Obviously, both the branching ratios and the direct CP asymmetries are related to the mixing angle.

In Table I, we present the input parameters used in the calculations, including the masses and decay constants of the mesons, the lifetime of the B^0 meson, and the Wolfenstein parameters of the CKM matrix elements [1, 4, 11, 47].

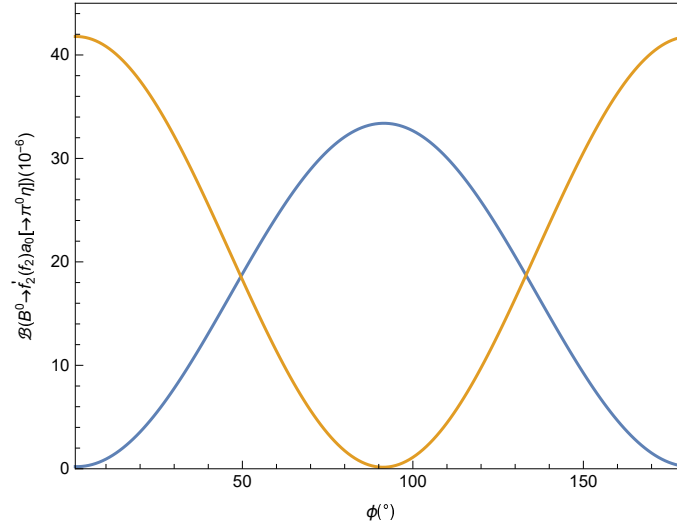
By using the helicity amplitudes and the input parameters, we predict the CP averaged branching fractions of the $B^0 \rightarrow TS[\rightarrow P_1 P_2]$ decays in the pQCD approach, and make some comments on the results. There are still many uncertainties in our calculation results. We primarily consider three types of errors. The first error is the decay constants of tensor mesons, the second is the shape parameter of B meson $\omega_b = 0.40 \pm 0.04$ GeV, and the third comes from the Gegenbauer coefficient $a_2 = 0.3 \pm 0.1$ for a_0 and $a_2 = 0.3 \pm 0.2$ for f_0 . We have neglected the uncertainties caused by the Wolfenstein parameters λ, A, ρ, η because they are typically small. In considered branching ratios, the major uncertainties stem from the shape parameter ω_b of the B meson's wave function and the Gegenbauer coefficient a_2 . It is well known that the S-wave two-meson distribution amplitudes are not well determined, this leads to significant errors in the Gegenbauer coefficient a_2 . The rigorous theoretical calculation for nonresonance contribution in the context of the PQCD framework is still absent, and the comparison between experiment measurements and theoretical predictions is still challenging. We hope that future research can further explore more precise description methods. It is worth mentioning that the ω_b plays vastly different roles in various decay modes. In Table II, the branching ratios of $B^0 \rightarrow K_2^{*0} a_0^0 [\rightarrow \pi^0 \eta, K^+ K^-]$ exhibit significantly higher sensitivity to the shape parameter ω_b than those of $B^0 \rightarrow K_2^{*+} a_0^- [\rightarrow \pi^- \eta, K^- K^0]$. Firstly, the contribution of the factorizable annihilation diagrams is unrelated to ω_b . Meanwhile, the $B^0 \rightarrow K_2^{*0} a_0^0 [\rightarrow \pi^0 \eta, K^+ K^-]$ and $B^0 \rightarrow K_2^{*+} a_0^- [\rightarrow \pi^- \eta, K^- K^0]$ are primarily dominated by tree operator

TABLE I. Input parameters of the $B^0 \rightarrow TS[\rightarrow P_1 P_2]$ decays

$M_B = 5.28 \text{ GeV}$	$m_b = 4.2 \text{ GeV}$	$f_B = 0.19 \pm 0.02 \text{ GeV}$	$\tau = 1.519 \text{ ps}$
$m_{a_0} = 0.98 \pm 0.02 \text{ GeV}$	$m_{f_0} = 0.99 \pm 0.02 \text{ GeV}$	$m_\sigma = 0.5 \text{ GeV}$	$\bar{f}_s = 0.37 \text{ GeV}$
$m_{K_2^{*0}} = 1.432 \text{ GeV}$	$M_{K_2^{*\pm}} = 1.427 \text{ GeV}$	$M_{a_2} = 1.317 \text{ GeV}$	$M_{f_2'} = 1.517 \text{ GeV}$
$M_{f_2} = 1.275 \text{ GeV}$	$f_{a_2} = 107 \pm 6 \text{ MeV}$	$f_{K_2^*} = 118 \pm 5 \text{ MeV}$	$f_{f_2} = 102 \pm 6 \text{ MeV}$
$f_{f_2'} = 126 \pm 4 \text{ MeV}$	$f_{a_2}^T = 105 \pm 21 \text{ MeV}$	$f_{K_2^*}^T = 77 \pm 14 \text{ MeV}$	$f_{f_2}^T = 117 \pm 25 \text{ MeV}$
$f_{f_2'}^T = 65 \pm 12 \text{ MeV}$	$m_{\pi^\pm} = 0.14 \text{ GeV}$	$m_{\pi^0} = 0.135 \text{ GeV}$	$m_{K^\pm} = 0.494 \text{ GeV}$
$m_{K^0} = 0.498 \text{ GeV}$	$m_\eta = 0.548 \text{ GeV}$		
$\lambda = 0.22650$	$A = 0.790$	$\bar{\rho} = 0.141$	$\bar{\eta} = 0.357$

contributions, and the nonfactorized emission diagrams will generate significant uncertainty from ω_b . However, the latter is suppressed by the coefficient $C1$, resulting in a relatively smaller impact from ω_b .

In Fig. 2 and Fig. 3, by setting the mixing angle ϕ to be a free parameter, we plot the variation of the branching fractions and direct CP asymmetries of decays $B^0 \rightarrow f_2' a_0^0 [\rightarrow \pi^0 \eta]$ and $B^0 \rightarrow f_2 a_0^0 [\rightarrow \pi^0 \eta]$ with the angle ϕ , respectively. In Fig. 2, the pattern of change in the decay branching ratio of $B^0 \rightarrow f_2' a_0^0 [\rightarrow \pi^0 \eta]$, indicated by the blue line, agrees with the image of the sine function, while the change in the decay branching ratio of $B^0 \rightarrow f_2 a_0^0 [\rightarrow \pi^0 \eta]$ with the mixing angle, indicated by the yellow line, satisfies the law of the cosine function. The detailed discussions about the mixing angle ϕ could be found in Refs[2, 4–7]. In Table II, we employ the most recent updated value 9° . It is known to us that the direct CP asymmetry is proportional to the interference between contributions from the tree and penguin operators. In Fig. 2 and Fig. 3, when the mixing angle $\phi = 0^\circ$, f_2' is regarded as the pure $s\bar{s}$, the branching ratio of $B^0 \rightarrow f_2' a_0^0 [\rightarrow \pi^0 \eta]$ is about 2.11×10^{-7} , the direct CP asymmetries are zero since it is pure penguin processes, and the both of value will increase a lot after considering the mixing of $\frac{1}{\sqrt{2}}(u\bar{u} + d\bar{d})$. Whereas for $B^0 \rightarrow f_2 a_0^0 [\rightarrow \pi^0 \eta]$ decay, the branching ratio is 4.18×10^{-5} with $\phi = 0^\circ$, the direct CP asymmetries are -2.57% and the values will have little change after considering the mixing of $s\bar{s}$. Moreover, in Table II, we find that the branching fractions of $B^0 \rightarrow f_2 a_0^0 [\rightarrow \pi^0 \eta]$ are 2 orders of magnitude larger than that of $B^0 \rightarrow f_2' a_0^0 [\rightarrow \pi^0 \eta]$. Therefore, $f_2^n = \frac{1}{\sqrt{2}}(u\bar{u} + d\bar{d})$ makes the dominant contribution in the decays, and $B^0 \rightarrow f_2' a_0^0 [\rightarrow \pi^0 \eta]$ are sensitive to the the interference between f_2^n and f_2^s .

FIG. 2. The branching ratio of $B^0 \rightarrow f_2'(f_2)a_0^0[\rightarrow \pi^0 \eta]$ decay with a variant of the mixing angle ϕ .

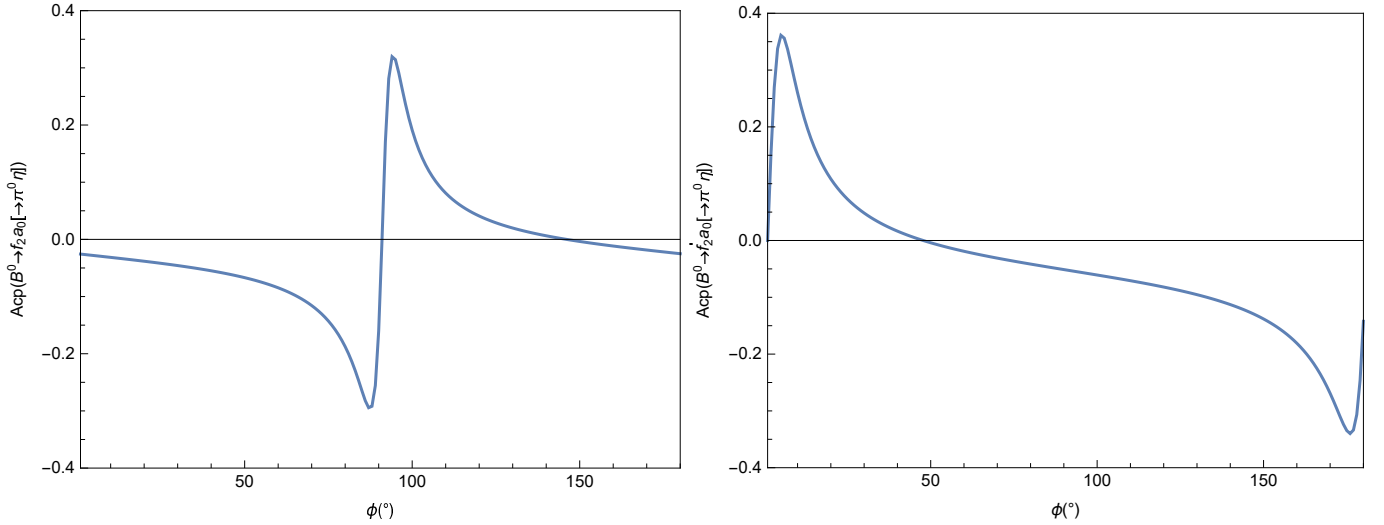


FIG. 3. The direct CP asymmetries of $B^0 \rightarrow f_2'(f_2)a_0^0[\rightarrow \pi^0\eta]$ with a variant of the mixing angle ϕ .

In Table II, we present the branching fractions and direct CP asymmetries of the $B^0 \rightarrow Ta_0[\rightarrow \pi\eta, K\bar{K}]$ decays. Meanwhile, we can find the branching ratios of the $B^0 \rightarrow Ta_0[\rightarrow \pi\eta]$ decays are much larger than that of the $B^0 \rightarrow Ta_0[\rightarrow K\bar{K}]a_0$ decays, which can be explained by the fact that the phase space for $K\bar{K}$ is suppressed. At the same time, the authors also concluded that the branching fractions of the $\pi\eta$ channel were five times larger than that of the $K\bar{K}$ channel with the resonance $a_0(980)$ in Ref. [47]. Next, we will use our calculations to investigate the value of $\Gamma(a_0 \rightarrow K^+K^-)/\Gamma(a_0 \rightarrow \pi^0\eta)$ with the narrow-width approximation.

When the narrow-width approximation is considered, the branching ratio of the quasi-two-body decay can be written as

$$\mathcal{B}(B \rightarrow M_1(R \rightarrow M_2M_3)) \simeq \mathcal{B}(B \rightarrow M_1R) \times \mathcal{B}(R \rightarrow M_2M_3), \quad (52)$$

with the resonance R . We can define a ratio \mathcal{R}_1 as

$$\mathcal{R}_1 = \frac{\Gamma(a_0 \rightarrow K^+K^-)}{\Gamma(a_0 \rightarrow \pi^0\eta)} = \frac{\mathcal{B}(B^0 \rightarrow Ta_0^0) \times \mathcal{B}(a_0^0 \rightarrow K^+K^-)}{\mathcal{B}(B^0 \rightarrow Ta_0^0) \times \mathcal{B}(a_0^0 \rightarrow \pi^0\eta)} \simeq \frac{\mathcal{B}(B^0 \rightarrow Ta_0^0[\rightarrow K^+K^-])}{\mathcal{B}(B^0 \rightarrow Ta_0^0[\rightarrow \pi^0\eta])}. \quad (53)$$

After considering the isospin relation $\Gamma(a_0 \rightarrow K^+K^-) = \Gamma(a_0 \rightarrow K\bar{K})/2$, we obtain the relative partial decay width

$$\frac{\Gamma(a_0 \rightarrow K\bar{K})}{\Gamma(a_0 \rightarrow \pi^0\eta)} \approx \begin{cases} 0.23 & K_2^*(1430) \\ 0.28 & a_2^0(1320) \\ 0.21 & f_2'(1525) \\ 0.22 & f_2(1270) \end{cases} \quad (54)$$

respectively. The OBELIX Collaboration acquired the ratio $\Gamma(a_0 \rightarrow K\bar{K})/\Gamma(a_0 \rightarrow \pi^0\eta) = 0.57 \pm 0.16$ using data from $\pi^+\pi^-\pi^0$, $K^+K^-\pi^0$, and $K^\pm K^0 S\pi^\mp$ [68]. In Ref. [69], the authors found the branching ratio for $\mathcal{B}(p\bar{p} \rightarrow a_0(980)\pi \rightarrow K\bar{K}\pi) = 5.92_{-1.01}^{+0.46} \times 10^{-4}$, and combined this with $\mathcal{B}(p\bar{p} \rightarrow a_0(980)\pi \rightarrow \pi^0\pi^0\eta) = (2.61 \pm 0.48) \times 10^{-4}$ [70], yielding $\Gamma(a_0 \rightarrow K\bar{K})/\Gamma(a_0 \rightarrow \pi\eta) = 0.23 \pm 0.05$. The WA102 Collaboration reported $\Gamma(a_0 \rightarrow K\bar{K})/\Gamma(a_0 \rightarrow \pi\eta) = 0.166 \pm 0.01 \pm 0.02$ from $f_1(1285)$ decays [71]. From this, it can be seen that for different decay processes, the analysis of the partial decay width ratio $\Gamma(a_0 \rightarrow K\bar{K})/\Gamma(a_0 \rightarrow \pi\eta)$ may yield some differences [46, 47, 72]. The Particle Data Group provides an average ratio of $\Gamma(a_0 \rightarrow K\bar{K})/\Gamma(a_0 \rightarrow \pi\eta) = 0.183 \pm 0.024$. Our results are slightly larger than this average but are consistent with the data from Ref. [69] within the errors.

The mixing angle θ is introduced into the $f_0 - \sigma$ mixing mechanism, which has not been determined precisely by current experimental measurements, and is suggested to be in the wide ranges of $25^\circ < \theta < 40^\circ$ [50, 73–75] and $135^\circ < \theta < 165^\circ$ [1, 10, 20, 22, 52]. In Figure 4 and Figure 5, by setting the mixing angle θ to be a free parameter, we plot the variation of the branching fractions and direct CP asymmetries of decays $B^0 \rightarrow K_2^* f_0(\sigma)[\rightarrow \pi^+\pi^-]$ and $B^0 \rightarrow a_2^0 f_0(\sigma)[\rightarrow \pi^+\pi^-]$ with the angle θ , respectively. In Figure 4, the pattern of change in the decay branching ratio of $B^0 \rightarrow K_2^* f_0[\rightarrow \pi^+\pi^-]$ and $B^0 \rightarrow a_2^0 f_0[\rightarrow \pi^+\pi^-]$, indicated by the blue line, the change in the decay branching ratio of $B^0 \rightarrow K_2^* \sigma[\rightarrow \pi^+\pi^-]$ and

TABLE II. CP -averaged branching fractions and the direct CP asymmetries for the $B^0 \rightarrow Ta_0[\rightarrow \pi\eta, K\bar{K}]$ decays in the pQCD approach.

Decay modes	\mathcal{B}	\mathcal{A}_{CP}
$B^0 \rightarrow K_2^*(1430)a_0^0[\rightarrow \pi^0\eta]$	$1.40^{+0.10+1.32+1.23}_{-0.07-0.64-0.81} \times 10^{-6}$	$-5.17^{+4.10+10.76+29.98}_{-4.61-6.49-13.33} \%$
$B^0 \rightarrow K_2^*(1430)a_0^0[\rightarrow K^+K^-]$	$1.64^{+0.10+1.51+1.40}_{-0.07-0.73-0.93} \times 10^{-7}$	$-3.73^{+4.34+9.31+29.27}_{-4.70-6.61-13.44} \%$
$B^0 \rightarrow K_2^{*+}(1430)a_0^-[\rightarrow \pi^-\eta]$	$2.78^{+0.34+0.50+1.03}_{-0.32-0.29-0.76} \times 10^{-7}$	$-35.80^{+1.66+0.93+2.18}_{-1.77-0.96-2.75} \%$
$B^0 \rightarrow K_2^{*+}(1430)a_0^-[\rightarrow K^-K^0]$	$5.25^{+0.70+1.02+2.12}_{-0.66-0.63-1.55} \times 10^{-8}$	$-41.82^{+1.71+2.36+2.22}_{-1.96-0.96-0.78} \%$
$B^0 \rightarrow a_2^0(1320)a_0^0[\rightarrow \pi^0\eta]$	$2.37^{+1.33+0.68+3.35}_{-1.01-0.35-1.88} \times 10^{-6}$	$-2.78^{+0.87+0.71+3.69}_{-1.44-0.11-12.63} \%$
$B^0 \rightarrow a_2^0(1320)a_0^0[\rightarrow K^+K^-]$	$3.33^{+1.48+1.45+4.54}_{-1.15-0.71-2.59} \times 10^{-7}$	$-3.90^{+0.97+0.87+3.75}_{-1.41-0.22-12.08} \%$
$B^0 \rightarrow a_2^+(1320)a_0^-[\rightarrow \pi^-\eta]$	$5.43^{+0.94+2.17+4.02}_{-0.86-1.41-2.88} \times 10^{-6}$	$11.57^{+0.52+1.44+4.07}_{-0.60-1.37-1.99} \%$
$B^0 \rightarrow a_2^+(1320)a_0^-[\rightarrow K^-K^0]$	$1.12^{+0.21+0.44+0.82}_{-0.18-0.28-0.58} \times 10^{-6}$	$11.82^{+0.62+1.34+3.93}_{-0.72-1.32-2.00} \%$
$B^0 \rightarrow a_2^-(1320)a_0^+[\rightarrow \pi^+\eta]$	$5.59^{+1.52+4.85+5.61}_{-0.21-3.60-3.18} \times 10^{-7}$	$13.84^{+12.93+0.29+17.48}_{-17.41-16.42-3.69} \%$
$B^0 \rightarrow a_2^-(1320)a_0^+[\rightarrow K^+K^0]$	$1.71^{+0.06+1.08+1.69}_{-0.01-0.87-1.03} \times 10^{-7}$	$-9.61^{+12.93+8.47+4.90}_{-8.99-18.54-2.83} \%$
$B^0 \rightarrow f_2'(1525)a_0^0[\rightarrow \pi^0\eta]$	$7.76^{+0.75+6.34+7.14}_{-0.67-3.43-4.76} \times 10^{-7}$	$28.53^{+3.55+2.83+1.51}_{-3.27-2.75-5.85} \%$
$B^0 \rightarrow f_2'(1525)a_0^0[\rightarrow K^+K^-]$	$8.21^{+0.78+6.79+7.59}_{-0.71-3.61-5.02} \times 10^{-8}$	$28.06^{+3.43+2.07+2.70}_{-3.22-2.22-9.46} \%$
$B^0 \rightarrow f_2(1270)a_0^0[\rightarrow \pi^0\eta]$	$4.10^{+0.83+3.18+3.27}_{-0.72-1.76-2.30} \times 10^{-5}$	$-3.08^{+1.60+0.53+1.56}_{-1.97-0.67-0.81} \%$
$B^0 \rightarrow f_2(1270)a_0^0[\rightarrow K^+K^-]$	$4.55^{+0.93+3.50+3.58}_{-0.80-1.96-2.53} \times 10^{-6}$	$-2.76^{+1.59+0.33+1.94}_{-2.00-0.44-1.00} \%$

$B^0 \rightarrow a_2^0\sigma[\rightarrow \pi^+\pi^-]$ with the mixing angle, indicated by the yellow line. We find graphically that the contribution from the $f_n = \frac{1}{\sqrt{2}}(u\bar{u} + d\bar{d})$ component is dominant. For these modes, both f_n and f_s will contribute, but the relative sign of the f_s state with respect to the f_n is negative for the σ and positive for the f_0 , which leads to a destructive interference between f_n and f_s for $B^0 \rightarrow K_2^*(a_2^0)\sigma[\rightarrow \pi^+\pi^-]$, but a constructive interference for $B^0 \rightarrow K_2^*(a_2^0)f_0[\rightarrow \pi^+\pi^-]$.

As we all known, both strong and weak phases are the necessary conditions for direct CP asymmetry. In Figure.5, we can observe when $\theta = 0^\circ$, the direct CP asymmetries of decay $B^0 \rightarrow K_2^*f_0[\rightarrow \pi^+\pi^-]$ is zero, since the decay is induced by $b \rightarrow ss\bar{s}$ transition. In the Wolfenstein parametrization of CKM matrix, there is no weak phase in this transition, which is a pure penguin process, the direct CP asymmetries is zero. For $B^0 \rightarrow K_2^*\sigma[\rightarrow \pi^+\pi^-]$ that is induced by $b \rightarrow sq\bar{q}(q = u, d)$, the direct CP asymmetries decay is less than 5%, because $|V_{us}V_{ub}| \ll |V_{ts}V_{tb}|$. Without the influence of mixing angles, the decay process $B^0 \rightarrow a_2^0f_0[\rightarrow \pi^+\pi^-]$ solely receives penguin contributions from the $c1$ and $d1$ nonfactorizable emission diagrams, resulting in a direct CP asymmetry of 0. Similarly, in the decay $B^0 \rightarrow a_2^0\sigma[\rightarrow \pi^+\pi^-]$, the interference between the tree and penguin contributions is minimal, yielding small direct CP asymmetries with 5.08%. However, when we incorporate mixing effects, the f_n term introduces tree contributions, thereby rendering the direct CP asymmetries of both $B^0 \rightarrow K_2^*f_0[\rightarrow \pi^+\pi^-]$ and $B^0 \rightarrow a_2^0f_0[\rightarrow \pi^+\pi^-]$ are no longer zero in this work. Therefore, if the two-quark structure will be confirmed, the branching fractions and CP asymmetries can be used to determine the mixing angle θ and study the nature of scalar particles.

In the current study, we take $\theta = 135^\circ, \phi = 9^\circ$ to make a numerical calculation and the Branching ratios and the direct CP asymmetries for the $B^0 \rightarrow Tf_0[\rightarrow \pi^+\pi^-, K^+K^-]$ and $B^0 \rightarrow T\sigma[\rightarrow \pi^+\pi^-]$ decays are presented in Table III. We can find that the direct CP asymmetries in the $B^0 \rightarrow Tf_0[\rightarrow \pi^+\pi^-]$ and $B^0 \rightarrow Tf_0[\rightarrow K^+K^-]$ decays with the same tensor are comparable. With the reason that the direct CP asymmetry is quantified by the ratio of decay rates, the impact of the scalar timelike form factor parameters and the invariant mass range in the quasi-two-body decay will be basically canceled. We still can find that the local CP asymmetries of the decays $B^0 \rightarrow K_2^*f_0[\rightarrow \pi^+\pi^-, K^+K^-]$ are as small as about 5%, and the reason is that the tree diagram contributions are both color and CKM elements suppressed. For the decay $B^0 \rightarrow a_2^0f_0[\rightarrow \pi^+\pi^-, K^+K^-]$, although the tree operator contributions proportional to the term $(C1 + C2/3)$ are color suppressed, the effects of penguin operators are significantly reduced due to the complete prohibition of factorizable diagrams involving emission tensors by Lorentz invariance, and the heavy suppression of factorizable diagrams for meson pair emission by the vector decay

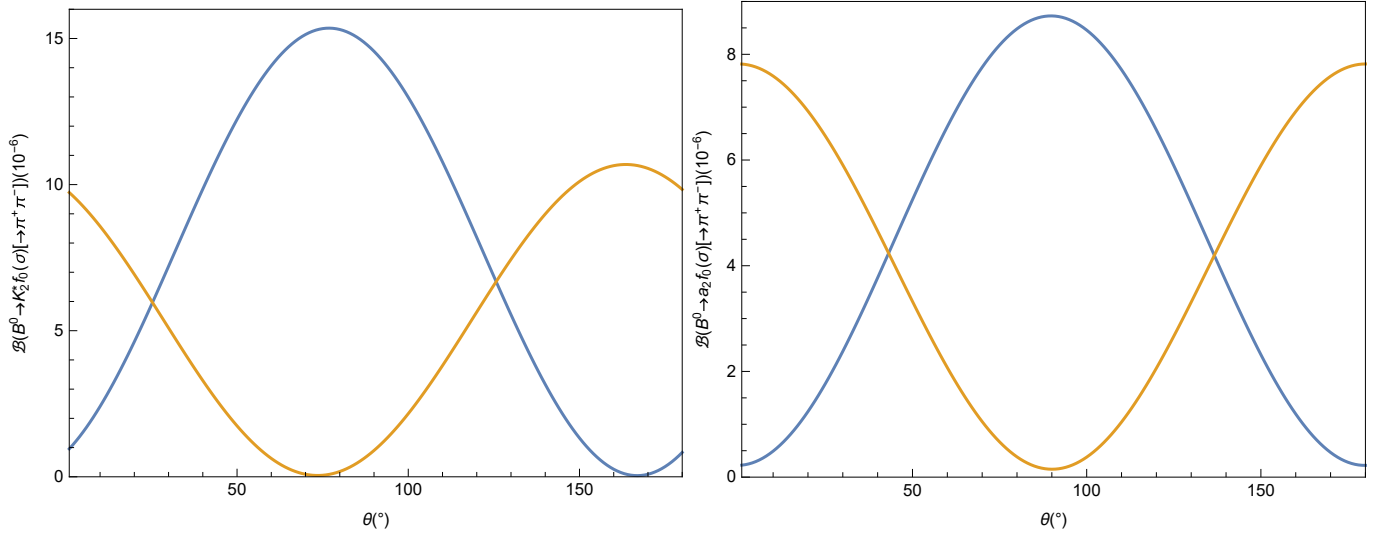


FIG. 4. The branching ratio of $B^0 \rightarrow K_2^* f_0(\sigma) [\rightarrow \pi^+ \pi^-]$ and $B^0 \rightarrow a_2^0 f_0(\sigma) [\rightarrow \pi^+ \pi^-]$ decay with variant of the mixing angle θ .

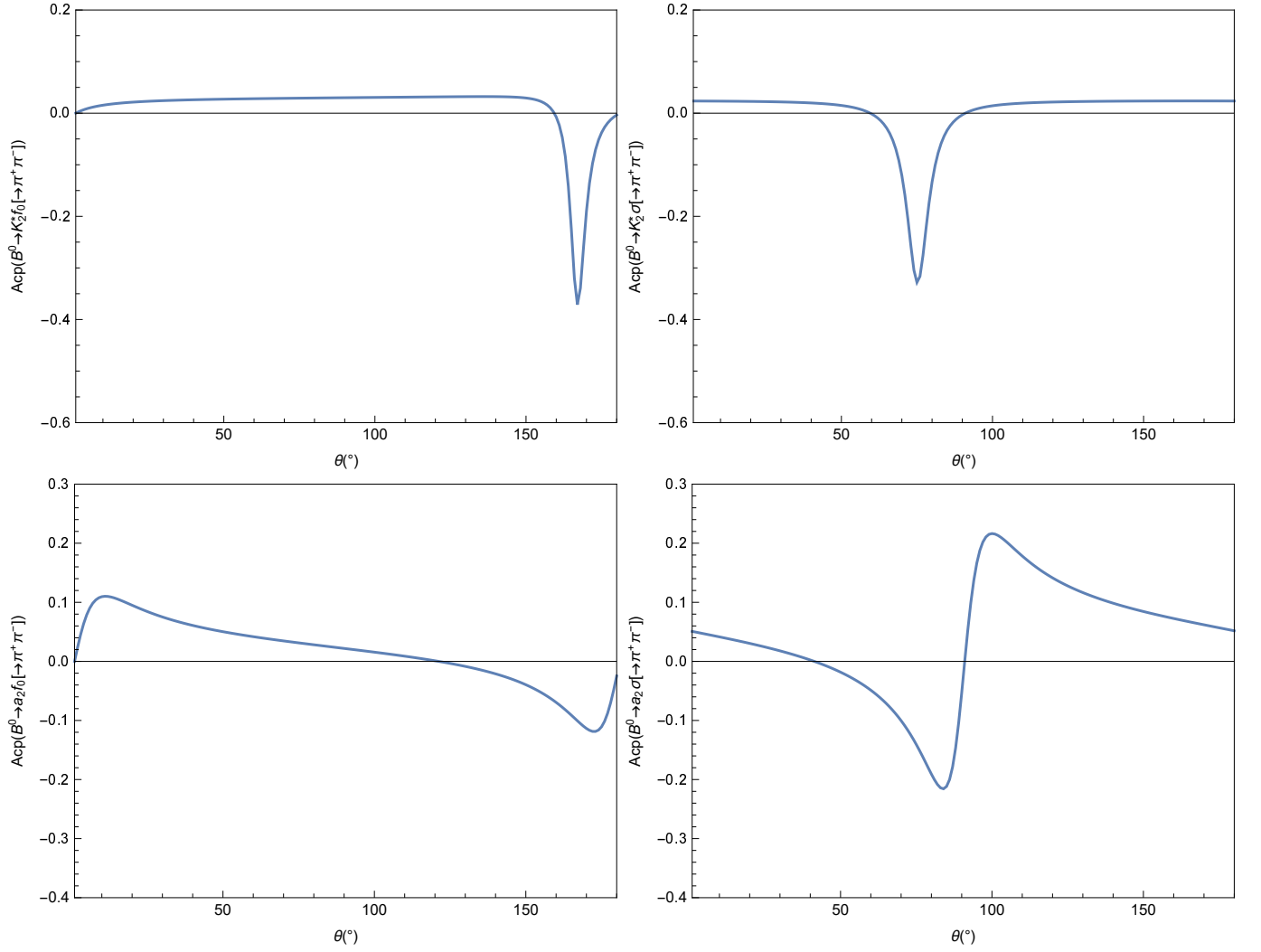


FIG. 5. The direct CP asymmetries of $B^0 \rightarrow K_2^* f_0(\sigma) [\rightarrow \pi^+ \pi^-]$ and $B^0 \rightarrow a_2^0 f_0(\sigma) [\rightarrow \pi^+ \pi^-]$ with variant of the mixing angle θ .

TABLE III. Branching ratios and the direct CP asymmetries for the $B^0 \rightarrow T f_0 [\rightarrow \pi^+ \pi^-, K^+ K^-]$ and $B^0 \rightarrow T \sigma [\rightarrow \pi^+ \pi^-] \sigma$ decays in the pQCD approach with the $f_0 - \sigma$ mixing angle $\theta = 135^\circ$.

Decay modes	\mathcal{B}	\mathcal{A}_{CP}
$B^0 \rightarrow K_2^*(1430) f_0 [\rightarrow \pi^+ \pi^-]$	$4.30^{+0.40+2.71+5.52}_{-0.34-1.57-3.21} \times 10^{-6}$	$3.21^{+2.95+2.30+3.02}_{-2.59-1.41-5.99} \%$
$B^0 \rightarrow K_2^*(1430) f_0 [\rightarrow K^+ K^-]$	$1.18^{+0.11+0.75+1.46}_{-0.09-0.43-0.86} \times 10^{-6}$	$6.13^{+2.83+1.89+2.66}_{-2.57-0.95-5.52} \%$
$B^0 \rightarrow K_2^*(1430) \sigma [\rightarrow \pi^+ \pi^-]$	$8.26^{+0.82+8.94+8.67}_{-0.51-4.24-3.88} \times 10^{-6}$	$1.63^{+0.40+0.36+0.20}_{-0.51-1.28-2.32} \%$
$B^0 \rightarrow a_2^0(1320) f_0 [\rightarrow \pi^+ \pi^-]$	$4.44^{+0.73+5.01+4.88}_{-0.57-2.39-2.09} \times 10^{-6}$	$-1.43^{+1.32+1.31+6.35}_{-1.08-0.38-0.37} \%$
$B^0 \rightarrow a_2^0(1320) f_0 [\rightarrow K^+ K^-]$	$1.02^{+0.14+1.15+1.14}_{-0.10-0.55-0.47} \times 10^{-6}$	$-1.39^{+1.53+1.62+6.06}_{-1.33-0.53-0.05} \%$
$B^0 \rightarrow a_2^0(1320) \sigma [\rightarrow \pi^+ \pi^-]$	$3.98^{+0.74+4.31+3.96}_{-0.61-2.09-1.83} \times 10^{-6}$	$10.69^{+2.69+2.20+1.00}_{-2.27-1.82-6.47} \%$
$B^0 \rightarrow f_2'(1525) f_0 [\rightarrow \pi^+ \pi^-]$	$1.10^{+0.04+0.61+1.28}_{-0.04-0.37-0.49} \times 10^{-7}$	$-72.69^{+7.63+2.66+23.46}_{-7.01-2.43-2.47} \%$
$B^0 \rightarrow f_2'(1525) f_0 [\rightarrow K^+ K^-]$	$2.51^{+0.12+1.43+2.96}_{-0.09-0.85-1.08} \times 10^{-8}$	$-72.39^{+8.26+1.43+48.09}_{-7.49-1.08-6.32} \%$
$B^0 \rightarrow f_2'(1525) \sigma [\rightarrow \pi^+ \pi^-]$	$3.77^{+0.09+3.78+4.16}_{-0.04-1.86-1.73} \times 10^{-8}$	$-94.94^{+3.21+7.81+50.55}_{-1.49-0.40-0.77} \%$
$B^0 \rightarrow f_2(1270) f_0 [\rightarrow \pi^+ \pi^-]$	$2.05^{+0.30+1.23+1.47}_{-0.16-0.79-0.77} \times 10^{-6}$	$19.47^{+4.01+0.58+7.18}_{-4.88-0.42-26.68} \%$
$B^0 \rightarrow f_2(1270) f_0 [\rightarrow K^+ K^-]$	$5.69^{+1.02+3.62+4.00}_{-0.61-2.28-2.07} \times 10^{-7}$	$14.28^{+4.25+0.28+7.65}_{-4.48-0.15-26.12} \%$
$B^0 \rightarrow f_2(1270) \sigma [\rightarrow \pi^+ \pi^-]$	$1.34^{+0.13+0.85+1.09}_{-0.02-0.52-0.55} \times 10^{-6}$	$-15.20^{+1.16+4.30+10.99}_{-0.39-3.00-3.91} \%$

constants of scalars from charge conjugation invariance. Consequently, the CP asymmetries observed in this decay process are indeed very small.

To compare with existing data and further discuss our calculations, we then use the narrow-width approximation to study the $B^0 \rightarrow K_2^* f_0 [\rightarrow \pi^+ \pi^-, K^+ K^-]$ decays which have the same resonance, we can define a ratio \mathcal{R}_2 to describe the relationship between $f_0 \rightarrow \pi^+ \pi^-$ and $f_0 \rightarrow K^+ K^-$, which can be given as

$$\mathcal{R}_2 = \frac{\mathcal{B}(f_0 \rightarrow K^+ K^-)}{\mathcal{B}(f_0 \rightarrow \pi^+ \pi^-)} = \frac{\mathcal{B}(B^0 \rightarrow K_2^* f_0) \times \mathcal{B}(f_0 \rightarrow K^+ K^-)}{\mathcal{B}(B^0 \rightarrow K_2^* f_0) \times \mathcal{B}(f_0 \rightarrow \pi^+ \pi^-)} \simeq \frac{\mathcal{B}(B^0 \rightarrow K_2^* f_0 [\rightarrow K^+ K^-])}{\mathcal{B}(B^0 \rightarrow K_2^* f_0 [\rightarrow \pi^+ \pi^-])} \approx 0.27, \quad (55)$$

This ratio can be used to estimate the branching ratios for the $f_0 \rightarrow \pi^+ \pi^-$ and $f_0 \rightarrow K^+ K^-$ decays by using the formulas $\mathcal{B}(f_0 \rightarrow \pi^+ \pi^-) = \frac{2}{4\mathcal{R}_2+3}$ and $\mathcal{B}(f_0 \rightarrow K^+ K^-) = \frac{2\mathcal{R}_2}{4\mathcal{R}_2+3}$ [76]. So we can get

$$\begin{aligned} \mathcal{B}(f_0 \rightarrow \pi^+ \pi^-) &\approx 0.49, \\ \mathcal{B}(f_0 \rightarrow K^+ K^-) &\approx 0.13. \end{aligned} \quad (56)$$

The BES Collaboration gained the relative branching ratios for the $\psi(2S) \rightarrow \gamma \chi_{c0}$ decays, where $\chi_{c0} \rightarrow f_0 f_0 \rightarrow \pi^+ \pi^- \pi^+ \pi^-$ or $\chi_{c0} \rightarrow f_0 f_0 \rightarrow \pi^+ \pi^- K^+ K^-$ [77, 78]. Meanwhile, the CLEO Collaboration has obtained $\mathcal{B}(f_0 \rightarrow K^+ K^-)/\mathcal{B}(f_0 \rightarrow \pi^+ \pi^-) = (25_{-11}^{+17})\%$ and extracted $\mathcal{B}(f_0 \rightarrow \pi^+ \pi^-) = (50_{-9}^{+7})\%$ by utilizing BES's findings [79]. Our calculations are well aligned with CLEO's results and theoretical outcomes [73, 74]. At the same time, based on the narrow width $\mathcal{B}(f_0 \rightarrow \pi^+ \pi^-) \approx 0.49$, we can evaluate $\mathcal{B}(B^0 \rightarrow K_2^* f_0) = 8.78 \times 10^{-6}$, which agree with the BABAR Collaboration's data [53] and theoretical results performed well in the two-body framework [10].

In Table III, the considered decays involving f_2' are sensitive to the ϕ , whereas the decays involving the f_2 are opposite. If there is no mixing in the $B^0 \rightarrow f_2' f_0 [\rightarrow \pi^+ \pi^-]$ decay process, the CP asymmetry is zero due to the pure penguin contribution from the annihilation diagram. However, when both the ϕ and θ mixing angles are taken into consideration simultaneously, they provide f_2^n and f_2^s components, leading to a significant interference between the tree operator contribution and the penguin contribution. This interference results in a large CP asymmetry and the branching ratio increases by 1 order of magnitude. The ϕ is really small, so the decay branching ratios involving f_2 barely change. The branching ratio of $B^0 \rightarrow f_2 f_0 [\rightarrow \pi^+ \pi^-]$ is

bigger than that of $B^0 \rightarrow f_2' f_0 [\rightarrow \pi^+ \pi^-]$ with the reason that the $\frac{1}{\sqrt{2}}(u\bar{u} + d\bar{d})$ component makes the dominant contribution in the B^0 decays.

In Ref. [52], the authors have taken the mixing angle $\theta = 145^\circ$, studied the branching fractions of the $B^0 \rightarrow V f_0 [\rightarrow \pi^+ \pi^-]$ decays in the pQCD approach, and gotten the results as follows:

$$\begin{aligned} \mathcal{B}(B^0 \rightarrow \rho^0 f_0 [\rightarrow \pi^+ \pi^-]) &= 0.82_{-0.34-0.16-0.10}^{+0.36+0.02+0.05} \times 10^{-6} \\ \mathcal{B}(B^0 \rightarrow \omega f_0 [\rightarrow \pi^+ \pi^-]) &= 0.97_{-0.39-0.19-0.10}^{+0.51+0.16+0.13} \times 10^{-6} \\ \mathcal{B}(B^0 \rightarrow K^{*0} f_0 [\rightarrow \pi^+ \pi^-]) &= 0.82_{-0.34-0.16-0.10}^{+0.36+0.02+0.05} \times 10^{-6} \end{aligned} \quad (57)$$

These are comparable to our results of $B^0 \rightarrow (a_2^0, f_2, K_2^*) f_0 [\rightarrow \pi^+ \pi^-]$ decays which are shown in Table III because ρ and a_2^0 , ω and f_2 , and K^{*0} and K_2^* have the same components in the quark model. The branching ratio of $B^0 \rightarrow (\rho^0, \omega, K^{*0}) f_0 [\rightarrow \pi^+ \pi^-]$ and $B^0 \rightarrow (a_2^0, f_2, K_2^*) f_0 [\rightarrow \pi^+ \pi^-]$ are at the same order but the former is a little small. The reason is that the QCD dynamics of the vector mesons and tensor mesons are different, the tensor meson has a greater mass than vector meson, and we take the smaller slightly mixing angle $\theta = 135^\circ$. As shown in Fig. 4, when the mixing angle $\theta > 90^\circ$, the contribution from the $\frac{1}{\sqrt{2}}(u\bar{u} + d\bar{d})$ component can cancel the contributions from the $s\bar{s}$ component, and the branching ratio of $B^0 \rightarrow T f_0 [\rightarrow \pi^+ \pi^-]$ decreases as the angle increases. We expect these results can be tested by the LHCb and Belle II experiments in the near future.

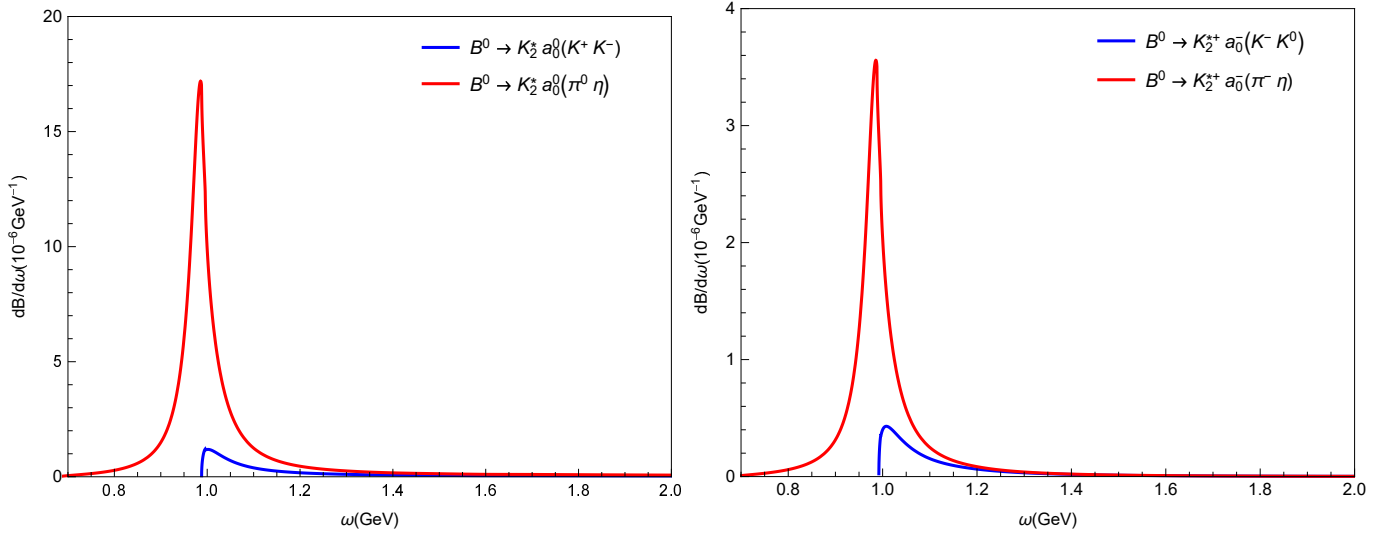


FIG. 6. Differential branching fractions of the $B^0 \rightarrow K_2^* a_0 [\rightarrow K\bar{K}, \pi\eta]$ decays.

Different from the fixed kinematics of the two-body decays, the decay amplitudes of the quasi-two-body decays depend on the invariant mass, which results in the differential distribution of branching ratios. In Fig. 6, we graph the differential branching ratios of the $B^0 \rightarrow K_2^* a_0 [\rightarrow K\bar{K}, \pi\eta]$ decays on the invariant mass; the results of the $B^0 \rightarrow K_2^* a_0^0 [\rightarrow K^+ K^-, \pi^0 \eta]$ models are shown on the left, and those of the $B^0 \rightarrow K_2^{*+} a_0^- [\rightarrow K^- K^0, \pi^- \eta]$ models are shown on the right. The differential branching ratios of the $B^0 \rightarrow K_2^* f_0 [\rightarrow \pi^+ \pi^-]$, $B^0 \rightarrow K_2^* f_0 [\rightarrow K^+ K^-]$, and $B^0 \rightarrow K_2^* \sigma [\rightarrow \pi^+ \pi^-]$ decays on the $\pi\pi$ or $K\bar{K}$ invariant mass ω are presented in Fig. 7 with a red solid line, blue solid line, or red dashed line, respectively. For the a_0 resonance, the contributions of the $K\bar{K}$ channel are much smaller than that of the $\pi\eta$ channel. From the figures, it is clear that the peak occurs around the resonance peak mass; the majority of the branching ratios are concentrated around the resonance state, basically in the range of $[m_S - \Gamma_S, m_S + \Gamma_S]$; and the contributions from the $\omega > 2.0 \text{ GeV}$ are really small and can be neglected safely.

IV. SUMMARY

In this article, considering the mixing angle $\theta = 135^\circ$ between $f_0(980)$ and $f_0(500)$, and $\phi = 9^\circ$ between $f_2(1270)$ and $f_2'(1525)$, we predict the branching fractions and direct CP asymmetries of the $B^0 \rightarrow T a_0 [\rightarrow K\bar{K}, \pi\eta]$, $B^0 \rightarrow T f_0 [\rightarrow \pi^+ \pi^-, K^+ K^-]$ and $B^0 \rightarrow T \sigma [\rightarrow \pi^+ \pi^-]$ decays with the pQCD approach firstly, where T denotes tensor mesons $a_2(1320)$, $K_2^*(1430)$, $f_2(1270)$, and $f_2'(1525)$; the scalars are considered as the $q\bar{q}$ state in the first scenario. Our results show that: among these considered decays, the pQCD predictions for the CP -averaged branching ratios vary in the range of 10^{-8} to 10^{-5} . The

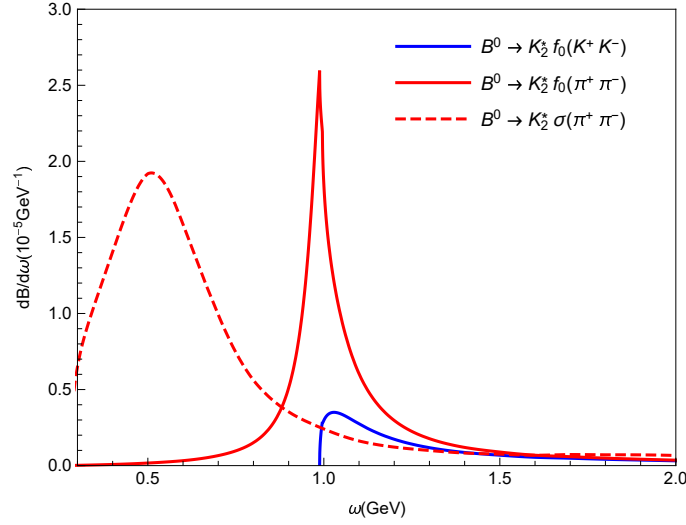


FIG. 7. Differential branching fractions of the $B^0 \rightarrow K_2^* f_0[\rightarrow \pi^+ \pi^-, K^+ K^-]$ and $B^0 \rightarrow K_2^* \sigma[\rightarrow \pi^+ \pi^-]$ decays.

branching fractions are sensitive to the θ , and the opposite is true for ϕ , except for some decays involving $f_2'(1525)$. The direct CP asymmetries are also affected by the mixing angle. Using the narrow-width approximation, we calculate the relative partial decay widths $\Gamma(a_0 \rightarrow K\bar{K})/\Gamma(a_0 \rightarrow \pi\eta)$ and the ratio $\mathcal{B}(f_0 \rightarrow K^+ K^-)/\mathcal{B}(f_0 \rightarrow \pi^+ \pi^-)$, and extract the decays $B^0 \rightarrow K_2^*(1430)^0 f_0(980)$ branching fractions, which are in agreement with the existing experimental and theoretical values. Our work has positive implications for understanding the QCD behavior of the scalars, and we also expect that our calculations can be tested by the LHCb and Belle II experiments in the future.

ACKNOWLEDGMENTS

This work is supported by the National Natural Science Foundation of China under Grant No.11047028.

APPENDIX : FACTORIZATION FORMULAS

In this section, we list the factorization formulas with $\bar{x}_i = 1 - x_i$, $\bar{\eta} = 1 - \eta$. $C_F = \frac{4}{3}$ stands for the color factor. Because of the charge conjugation invariance, the S -wave meson pair cannot be emitted with the $(\bar{V} - A)(V - A)$ and $(V - A)(V + A)$ current, namely

$$F_S^{LL} = F_S^{LR} = 0 \quad (\text{A.1})$$

$$\begin{aligned} F_S^{SP} = & 16\sqrt{\frac{2}{3}}\pi C_F \bar{f}_s M_B^4 \int_0^1 dx_B dx_3 \int_0^\infty b_B db_B b_3 db_3 \phi_B(x_B, b_B) \\ & \times \{ [rx_3\bar{\eta}(r^2 - \bar{\eta})\phi_T^t + r(4r_b - 2 + x_3(r^2 + \bar{\eta}))\phi_T^s + (\bar{\eta} - r^2)(2 - r_b)\phi_T] \\ & \times \alpha_s(t_{a1})h_{a1}(\alpha_{a1}, \beta_{a1}, b_B, b_3) \exp[-S_B(t_{a1}) - S_3(t_{a1})]S_t(x_3) \\ & + [2r(\bar{\eta} - x_B + r^2)\phi_T^s - r^2 x_B \phi_T] \alpha_s(t_{b1})h_{b1}(\alpha_{b1}, \beta_{b1}, b_3, b_B) \exp[-S_B(t_{b1}) - S_3(t_{b1})]S_t(x_B) \}. \end{aligned} \quad (\text{A.2})$$

$$\begin{aligned} M_S^{LL} = & -\frac{32}{3}\pi C_F M_B^4 \int_0^1 dx_B dz dx_3 \int_0^\infty b_B db_B b db \phi_B(x_B, b_B) \phi_S \\ & \times \{ [r((r^2 - 1)(x_B + (z - 2)\eta) + x_3\bar{\eta} + r^2 x_3(2\eta - 1))\phi_T^s + r\bar{\eta}((1 - r^2)(x_B - z\eta) + x_3(r^2 - \bar{\eta}))\phi_T^t \\ & + (r^2 - 1 - \eta)(z\bar{\eta} + r^2(z\bar{\eta} - \bar{x}_B))\phi_T] \alpha_s(t_{c1})h_{c1}(\alpha_{c1}, \beta_{c1}, b, b_B) \exp[-S_B(t_{c1}) - S(t_{c1}) - S_3(t_{c1})] \\ & + [r((r^2 - 1)(x_B - z\eta) + x_3\bar{\eta} + r^2 x_3(2\eta - 1))\phi_T^s + r\bar{\eta}((r^2 - 1)(x_B + z\eta) - x_3(r^2 - \bar{\eta}))\phi_T^t \\ & + (r^2 - 1 + \eta)((1 - r^2)z - x_B + x_3(r^2 + \bar{\eta}))\phi_T] \alpha_s(t_{d1})h_{d1}(\alpha_{d1}, \beta_{d1}, b, b_B) \exp[-S_B(t_{d1}) - S(t_{d1}) - S_3(t_{d1})] \} \end{aligned} \quad (\text{A.3})$$

$$\begin{aligned}
M_S^{LR} = & -\frac{32}{3}\pi C_F M_B^4 \int_0^1 dx_B dz dx_3 \int_0^\infty b_B db_B b db \phi_B(x_B, b_B) \\
& \times \{ [2(\bar{z} + r^2(x_3 - \bar{z}))(\bar{\eta}\phi_T + r\phi_T^s - r\bar{\eta}\phi_T^t)\phi_S^t + ((\bar{z}\bar{\eta} + r^2(z\bar{\eta} - \bar{x}_B))\phi_T \\
& + r(\bar{x}_B - z + x_3 + r^2(x_3 - \bar{z}) + \bar{x}_3\eta)\phi_T^s - r\bar{\eta}(\bar{x}_3\bar{\eta} + x_B - z + r^2(x_3 - \bar{z}))\phi_T^t)(\phi_S^s - \phi_S^t)] \\
& \times \alpha_s(t_{c1})h_{c1}(\alpha_{c1}, \beta_{c1}, b, b_B) \exp[-S_B(t_{c1}) - S(t_{c1}) - S_3(t_{c1})] - [2r(x_B - x_3\bar{\eta})(r\phi_T - \phi_T^s - \bar{\eta}\phi_T^t)\phi_S^t \\
& + ((\bar{z}\bar{\eta} + r^2(x_B - z\bar{\eta}))\phi_T + r(z(1 - r^2) - x_B + x_3(\bar{\eta} + r^2))\phi_T^s - r\bar{\eta}(z(1 - r^2) + x_B + x_3(r^2 - \bar{\eta}))\phi_T^t) \\
& \times (\phi_S^s - \phi_S^t)]\alpha_s(t_{d1})h_{d1}(\alpha_{d1}, \beta_{d1}, b, b_B) \exp[-S_B(t_{d1}) - S(t_{d1}) - S_3(t_{d1})] \}
\end{aligned} \tag{A.4}$$

$$\begin{aligned}
M_S^{SP} = & -\frac{32}{3}\pi C_F M_B^4 \int_0^1 dx_B dz dx_3 \int_0^\infty b_B db_B b db \phi_B(x_B, b_B) \phi_S \\
& \times \{ [r((r^2 - 1)(x_B + (z - 2)\eta) + x_3\bar{\eta} + r^2 x_3(2\eta - 1))\phi_T^s - r\bar{\eta}((1 - r^2)(x_B - z\eta) + x_3(r^2 - \bar{\eta}))\phi_T^t \\
& + (r^2 - \bar{\eta})(\bar{x}_B + x_3 - z + r^2(x_3 - \bar{z}) + \eta\bar{x}_3)\phi_T]\alpha_s(t_{c1})h_{c1}(\alpha_{c1}, \beta_{c1}, b, b_B) \exp[-S_B(t_{c1}) - S(t_{c1}) - S_3(t_{c1})] \\
& - [r((r^2 - 1)(x_B - z\eta) + x_3\bar{\eta} + r^2 x_3(2\eta - 1))\phi_T^s - r\bar{\eta}((r^2 - 1)(x_B + z\eta) - x_3(r^2 - \bar{\eta}))\phi_T^t \\
& + (r^2 - 1 - \eta)(z\bar{\eta} + r^2(x_B - z\bar{\eta}))\phi_T]\alpha_s(t_{d1})h_{d1}(\alpha_{d1}, \beta_{d1}, b, b_B) \exp[-S_B(t_{d1}) - S(t_{d1}) - S_3(t_{d1})] \}
\end{aligned} \tag{A.5}$$

$$\begin{aligned}
A_S^{LL} = & 8\sqrt{\frac{2}{3}}\pi C_F f_B M_B^4 \int_0^1 dz dx_3 \int_0^\infty b db b_3 db_3 \\
& \times \{ [2r\sqrt{(1 - r^2)}\eta x_3\bar{\eta}(\bar{\eta} - r^2)\phi_S^s\phi_T^t - 2r\sqrt{(1 - r^2)}\eta(x_3(r^2 + \bar{\eta}) - 2)\phi_S^s\phi_T^s \\
& + (\bar{\eta} - r^2)(x_3\bar{\eta} - 1 + r^2 x_3\eta)\phi_S\phi_T]\alpha_s(t_{e1})h_{e1}(\alpha_{e1}, \beta_{e1}, b, b_3) \exp[-S_3(t_{e1}) - S(t_{e1})]S_t(x_3) \\
& - [2r\sqrt{(1 - r^2)}\eta(r^2\bar{z} - \bar{z} + \eta)\phi_S^t\phi_T^s + 2r\sqrt{(1 - r^2)}\eta(r^2\bar{z} + z + \bar{\eta})\phi_S^s\phi_T^s \\
& + \bar{\eta}(r^4\bar{z} - z + r^2(2z - \bar{\eta}))\phi_S\phi_T]\alpha_s(t_{f1})h_{f1}(\alpha_{f1}, \beta_{f1}, b_3, b) \exp[-S_3(t_{f1}) - S(t_{f1})]S_t(z) \}
\end{aligned} \tag{A.6}$$

$$A_S^{LR} = A_S^{LL} \tag{A.7}$$

$$\begin{aligned}
A_S^{SP} = & -16\sqrt{\frac{2}{3}}\pi C_F f_B M_B^4 \int_0^1 dz dx_3 \int_0^\infty b db b_3 db_3 \\
& \times \{ [r(x_3\bar{\eta} - 1 - \eta + r^2(\bar{x}_3 + 2\eta x_3))\phi_S\phi_T^s - 2\sqrt{(1 - r^2)}\eta(r^2 - \bar{\eta})\phi_S^s\phi_T \\
& + r\bar{x}_3\bar{\eta}(r^2 - \bar{\eta})\phi_S\phi_T^t]\alpha_s(t_{e1})h_{e1}(\alpha_{e1}, \beta_{e1}, b, b_3) \exp[-S_3(t_{e1}) - S(t_{e1})]S_t(x_3) \\
& - [2r^2\sqrt{(1 - r^2)}\eta\bar{\eta}\phi_S^t\phi_T - 2r(\bar{z}\eta - 1 + r^2(1 - 2\eta + z\eta))\phi_S\phi_T^s \\
& + \sqrt{(1 - r^2)}\eta(r^2 - 1)z\bar{\eta}(\phi_S^s - \phi_S^t)\phi_T]\alpha_s(t_{f1})h_{f1}(\alpha_{f1}, \beta_{f1}, b_3, b) \exp[-S_3(t_{f1}) - S(t_{f1})]S_t(z) \}
\end{aligned} \tag{A.8}$$

$$\begin{aligned}
W_S^{LL} = & -\frac{32}{3}\pi C_F M_B^4 \int_0^1 dx_B dz dx_3 \int_0^\infty b_B db_B b db \phi_B(x_B, b_B) \\
& \times \{ [(r_b(\bar{\eta} - r^2) + (1 - r^2 + \eta)(\eta - \bar{z} + r^2(\bar{z} - x_B) + (r^2 - 1)z\eta))\phi_S\phi_T + 2r\sqrt{(1 - r^2)}\eta(\bar{z} + r^2(x_3 - \bar{z})) \\
& \times \phi_S^t(\phi_T^s - \bar{\eta}\phi_T^t) + r\sqrt{(1 - r^2)}\eta(\bar{x}_B + x_3 - z + r^2(x_3 - \bar{z}) + \bar{x}_3\eta)(\phi_S^s - \phi_S^t)\phi_T^s - 4rr_b\sqrt{(1 - r^2)}\eta\phi_S^s\phi_T^s \\
& - r\bar{\eta}\sqrt{(1 - r^2)}\eta(x_B - z + r^2(x_3 - \bar{z}) + \bar{x}_3\bar{\eta})(\phi_S^s - \phi_S^t)\phi_T^t]\alpha_s(t_{g1})h_{g1}(\alpha_{g1}, \beta_{g1}, b_B, b) \\
& \times \exp[-S_B(t_{g1}) - S(t_{g1}) - S_3(t_{g1})] - [2r\sqrt{(1 - r^2)}\eta(x_B - \bar{x}_3\bar{\eta})\phi_S^t(\phi_T^s - \bar{\eta}\phi_T^t) \\
& + (r^2 - \bar{\eta})(x_B - \bar{x}_3\bar{\eta} - z\eta - r^2(x_B - \bar{x}_3(1 - 2\eta) - z\eta))\phi_S\phi_T \\
& + r\sqrt{(1 - r^2)}\eta(x_B - \bar{x}_3\bar{\eta} + r^2(x_3 - \bar{z}) - z)(\phi_S^s - \phi_S^t)\phi_T^s + r\bar{\eta}\sqrt{(1 - r^2)}\eta(\bar{x}_3\bar{\eta} - x_B + r^2(x_3 - \bar{z}) - z) \\
& \times (\phi_S^s - \phi_S^t)\phi_T^t]\alpha_s(t_{h1})h_{h1}(\alpha_{h1}, \beta_{h1}, b_B, b) \exp[-S_B(t_{h1}) - S(t_{h1}) - S_3(t_{h1})] \}
\end{aligned} \tag{A.9}$$

$$\begin{aligned}
W_S^{LR} = & -\frac{32}{3}\pi C_F M_B^4 \int_0^1 dx_B dz dx_3 \int_0^\infty b_B db_B b db \phi_B(x_B, b_B) \\
& \times \{ [2\bar{\eta}\sqrt{(1-r^2)}\eta(\bar{z}+r^2(x_3-\bar{z})+r_b)\phi_S^t\phi_T + r((1-r^2)(r_b-x_B+x_3)+(2+r_b-z-x_3+r^2(z-2\bar{x}_3))\eta) \\
& \times \phi_S\phi_T^s - \sqrt{(1-r^2)}\eta(r^2(\bar{x}_B+r_b-z\bar{\eta})-(r_b+\bar{z})\bar{\eta})(\phi_S^s-\phi_S^t)\phi_T + r\bar{\eta}((1-r^2)(x_B-z\eta)+(x_3+r_b)(r^2-\bar{\eta})) \\
& \times \phi_S\phi_T^t] \alpha_s(t_{g1}) h_{g1}(\alpha_{g1}, \beta_{g1}, b_B, b) \exp[-S_B(t_{g1}) - S(t_{g1}) - S_3(t_{g1})] \\
& - [2\bar{\eta}\sqrt{(1-r^2)}\eta(r^2(x_3-\bar{z})-z)\phi_S^t\phi_T - r(\bar{x}_3\bar{\eta}-x_B+z\eta+r^2(x_B-(1-2\eta)\bar{x}_3-z\eta))\phi_S\phi_T^s \\
& - \sqrt{(1-r^2)}\eta(z\bar{\eta}+r^2(x_B-z\bar{\eta}))(\phi_S^s-\phi_S^t)\phi_T + r\bar{\eta}(\bar{x}_3\bar{\eta}-x_B+r^2(x_3-\bar{x}_B+z\eta)-z\eta)\phi_S\phi_T^t] \\
& \times \alpha_s(t_{h1}) h_{h1}(\alpha_{h1}, \beta_{h1}, b_B, b) \exp[-S_B(t_{h1}) - S(t_{h1}) - S_3(t_{h1})] \} \quad (A.10)
\end{aligned}$$

$$\begin{aligned}
W_S^{SP} = & \frac{32}{3}\pi C_F M_B^4 \int_0^1 dx_B dz dx_3 \int_0^\infty b_B db_B b db \phi_B(x_B, b_B) \\
& \times \{ [(r^2-\bar{\eta})(r_b+(1-r^2)(x_B-x_3)+(z-2+x_3-r^2(z-2\bar{x}_3))\eta)\phi_S\phi_T + 2r\sqrt{(1-r^2)}\eta(x_B-x_3\bar{\eta}-\eta) \\
& \times \phi_S^t(\phi_T^s-\bar{\eta}\phi_T^t) + 4rr_b\sqrt{(1-r^2)}\eta\phi_S^s\phi_T^s - r\bar{\eta}\sqrt{(1-r^2)}\eta(x_B+\bar{x}_3\bar{\eta}-z+r^2(x_3-\bar{z}))(\phi_S^s-\phi_S^t)\phi_T^t \\
& - r\sqrt{(1-r^2)}\eta(\bar{x}_B+x_3-z+r^2(x_3-\bar{z})+\bar{x}_3\eta)(\phi_S^s-\phi_S^t)\phi_T^s] \alpha_s(t_{g1}) h_{g1}(\alpha_{g1}, \beta_{g1}, b_B, b) \exp[-S_B(t_{g1}) \\
& - S(t_{g1}) - S_3(t_{g1})] - [r\bar{\eta}\sqrt{(1-r^2)}\eta(\bar{x}_3\bar{\eta}-x_B-z+r^2(x_3-\bar{z}))(\phi_S^s-\phi_S^t)\phi_T^t - 2r\sqrt{(1-r^2)}\eta(r^2(x_3-\bar{z}) \\
& - z)\phi_S^t(\phi_T^s-\bar{\eta}\phi_T^t) + (r^2-1-\eta)(z\bar{\eta}+r^2(x_B-z\bar{\eta}))\phi_S\phi_T - r\sqrt{(1-r^2)}\eta(x_B-\bar{x}_3\bar{\eta}-z+r^2(x_3-\bar{z})) \\
& \times (\phi_S^s-\phi_S^t)\phi_T^s] \alpha_s(t_{h1}) h_{h1}(\alpha_{h1}, \beta_{h1}, b_B, b) \exp[-S_B(t_{h1}) - S(t_{h1}) - S_3(t_{h1})] \} \quad (A.11)
\end{aligned}$$

$$\begin{aligned}
M_T^{LL} = & -\frac{32}{3}\pi C_F M_B^4 \int_0^1 dx_B dz dx_3 \int_0^\infty b_B db_B b_3 db_3 \phi_B(x_B, b_B) \phi_T \\
& \times \{ [2r^2\sqrt{(1-r^2)}\eta(x_B-\bar{x}_3\bar{\eta})\phi_S^t + \sqrt{(1-r^2)}\eta(z\bar{\eta}+r^2(x_B-z\bar{\eta}))(\phi_S^s-\phi_S^t) + (\bar{\eta}-r^2) \\
& \times (x_B-\bar{x}_3\bar{\eta}-z\eta-r^2(x_B-\bar{x}_3+2\eta\bar{x}_3-z\eta))\phi_S] \alpha_s(t_{c2}) h_{c2}(\alpha_{c2}, \beta_{c2}, b_3, b_B) \exp[-S_B(t_{c2}) - S(t_{c2}) \\
& - S_3(t_{c2})] - [\sqrt{(1-r^2)}\eta(z\bar{\eta}+r^2(x_B-z\bar{\eta}))(\phi_S^s-\phi_S^t) - 2\bar{\eta}\sqrt{(1-r^2)}\eta(z(r^2-1)-r^2x_3)\phi_S^t + (\bar{\eta}-r^2) \\
& \times (x_B+z(r^2-1)-(\bar{\eta}+r^2)x_3)\phi_S] \alpha_s(t_{d2}) h_{d2}(\alpha_{d2}, \beta_{d2}, b_3, b_B) \exp[-S_B(t_{d2}) - S(t_{d2}) - S_3(t_{d2})] \} \quad (A.12)
\end{aligned}$$

$$\begin{aligned}
M_T^{LR} = & -\frac{32}{3}\pi C_F M_B^4 \int_0^1 dx_B dz dx_3 \int_0^\infty b_B db_B b_3 db_3 \phi_B(x_B, b_B) \\
& \times \{ [2\sqrt{(1-r^2)}\eta(z-r^2(x_3-\bar{z}))\phi_S^t(\phi_T^s-\bar{\eta}\phi_T^t) + (\bar{x}_3\bar{\eta}-x_B+z\eta+r^2(x_B-\bar{x}_3+2\eta\bar{x}_3-z\eta))\phi_S\phi_T^s \\
& - \sqrt{(1-r^2)}\eta(x_B-\bar{x}_3\bar{\eta}-z+r^2(x_3-\bar{z}))(\phi_S^s-\phi_S^t)\phi_T^t + \bar{\eta}(\bar{x}_3\bar{\eta}-x_B-z\eta+r^2(x_B-\bar{x}_3+z\eta))\phi_S\phi_T^t \\
& + \bar{\eta}\sqrt{(1-r^2)}\eta(\bar{x}_3\bar{\eta}-x_B-z+r^2(x_3-\bar{z}))(\phi_S^s-\phi_S^t)\phi_T^t] \alpha_s(t_{c2}) h_{c2}(\alpha_{c2}, \beta_{c2}, b_3, b_B) \exp[-S_B(t_{c2}) \\
& - S(t_{c2}) - S_3(t_{c2})] - [((r^2-1)(x_B-z\eta)+x_3\bar{\eta}+r^2x_3(2\eta-1))\phi_S\phi_T^s - 2\sqrt{(1-r^2)}\eta(z(r^2-1)-r^2x_3) \\
& \times \phi_S^t(\phi_T^s+\bar{\eta}\phi_T^t) - \bar{\eta}((r^2-1)(x_B+z\eta-x_3)-x_3\eta)\phi_S\phi_T^t - \sqrt{(1-r^2)}\eta(x_B+z(r^2-1)-(r^2+\bar{\eta})x_3) \\
& \times (\phi_S^s-\phi_S^t)\phi_T^t + \bar{\eta}\sqrt{(1-r^2)}\eta(x_B+(1-r^2)(z-x_3)+x_3\eta)(\phi_S^s-\phi_S^t)\phi_T^t] \\
& \times \alpha_s(t_{d2}) h_{d2}(\alpha_{d2}, \beta_{d2}, b_3, b_B) \exp[-S_B(t_{d2}) - S(t_{d2}) - S_3(t_{d2})] \} \quad (A.13)
\end{aligned}$$

$$\begin{aligned}
M_T^{SP} = & -\frac{32}{3}\pi C_F M_B^4 \int_0^1 dx_B dz dx_3 \int_0^\infty b_B db_B b_3 db_3 \phi_B(x_B, b_B) \phi_T \\
& \times \{ [\sqrt{(1-r^2)}\eta(z\bar{\eta}+r^2(x_B-z\bar{\eta}))(\phi_S^s-\phi_S^t) - 2\bar{\eta}\sqrt{(1-r^2)}\eta(r^2(x_3-\bar{z})-z)\phi_S^t \\
& + (\bar{\eta}-r^2)(x_B-\bar{x}_3\bar{\eta}-z+r^2(x_3-\bar{z}))\phi_S] \alpha_s(t_{c2}) h_{c2}(\alpha_{c2}, \beta_{c2}, b_3, b_B) \exp[-S_B(t_{c2}) - S(t_{c2}) - S_3(t_{c2})] \\
& - [2r^2\sqrt{(1-r^2)}\eta(x_B-x_3\bar{\eta})\phi_S^t + \sqrt{(1-r^2)}\eta(z\bar{\eta}+r^2(x_B-z\bar{\eta}))(\phi_S^s-\phi_S^t) + (r^2-\bar{\eta}) \\
& \times ((r^2-1)(x_B-z\eta)+x_3\bar{\eta}+r^2x_3(2\eta-1))\phi_S] \alpha_s(t_{d2}) h_{d2}(\alpha_{d2}, \beta_{d2}, b_3, b_B) \exp[-S_B(t_{d2}) - S(t_{d2}) - S_3(t_{d2})] \} \quad (A.14)
\end{aligned}$$

$$\begin{aligned}
A_T^{LL} = & 8\sqrt{\frac{2}{3}}\pi C_F f_B M_B^4 \int_0^1 dz dx_3 \int_0^\infty b db b_3 db_3 \\
& \times \{ [2r\sqrt{(1-r^2)}\eta(2+(r^2-1)z)(\phi_S^s - \phi_S^t)\phi_T^s - (\bar{z}\bar{\eta} + r^2(2z\bar{\eta} - 1) - r^4 z\bar{\eta})\phi_S\phi_T \\
& + 4r\sqrt{(1-r^2)}\eta\phi_S^t\phi_T^s]\alpha_s(t_{e2})h_{e2}(\alpha_{e2}, \beta_{e2}, b_3, b) \exp[-S_3(t_{e2}) - S(t_{e2})]S_t(z) \\
& - [(r^2 - \bar{\eta})(x_3 + (1-r^2)\bar{x}_3\eta)\phi_S\phi_T + 2r\sqrt{(1-r^2)}\eta(1+x_3-r^2\bar{x}_3+\bar{x}_3\eta)\phi_S^s\phi_T^s \\
& + 2r\sqrt{(1-r^2)}\eta\bar{x}_3\bar{\eta}(r^2 - \bar{\eta})\phi_S^s\phi_T^t]\alpha_s(t_{f2})h_{f2}(\alpha_{f2}, \beta_{f2}, b, b_3) \exp[-S_3(t_{f2}) - S(t_{f2})]S_t(x_3) \}
\end{aligned} \tag{A.15}$$

$$A_T^{LR} = A_T^{LL} \tag{A.16}$$

$$\begin{aligned}
A_T^{SP} = & -16\sqrt{\frac{2}{3}}\pi C_F f_B M_B^4 \int_0^1 dz dx_3 \int_0^\infty b db b_3 db_3 \\
& \times \{ [\sqrt{(1-r^2)}\eta(r^2(1-z\bar{\eta}) - \bar{\eta}\bar{z})(\phi_S^s - \phi_S^t)\phi_T - 2\bar{\eta}\sqrt{(1-r^2)}\eta(1+(r^2-1)z)\phi_S^t\phi_T \\
& + 2r(1+\bar{z}\eta+r^2(z\eta-1))\phi_S\phi_T^s]\alpha_s(t_{e2})h_{e2}(\alpha_{e2}, \beta_{e2}, b_3, b) \exp[-S_3(t_{e2}) - S(t_{e2})]S_t(z) \\
& + [2\sqrt{(1-r^2)}\eta(r^2 - \bar{\eta})\phi_S^s\phi_T + r(x_3\bar{\eta} - 2(r^2-1)\eta + r^2 x_3(2\eta-1))\phi_S\phi_T^s \\
& + r x_3\bar{\eta}(r^2 - \bar{\eta})\phi_S\phi_T^t]\alpha_s(t_{f2})h_{f2}(\alpha_{f2}, \beta_{f2}, b, b_3) \exp[-S_3(t_{f2}) - S(t_{f2})]S_t(x_3) \}
\end{aligned} \tag{A.17}$$

$$\begin{aligned}
W_T^{LL} = & -\frac{32}{3}\pi C_F M_B^4 \int_0^1 dx_B dz dx_3 \int_0^\infty b_B db_B b_3 db_3 \phi_B(x_B, b_B) \\
& \times \{ [r\sqrt{(1-r^2)}\eta(\bar{x}_3\bar{\eta} - x_B - z + r^2(x_3 - \bar{z}))(\phi_S^s - \phi_S^t)\phi_T^t - (x_B - \bar{x}_3\bar{\eta} - z + r^2(x_3 - \bar{z}))(\phi_S^s - \phi_S^t)\phi_T^s \\
& - 2(r^2(x_3 - \bar{z}) - z)\phi_S^t(\phi_T^s - \bar{\eta}\phi_T^t) - (r_b + x_B - \bar{x}_3\bar{\eta} - z\eta - r^2(x_B + (2\eta-1)\bar{x}_3 - z\eta)) \\
& \times (r^2 - \bar{\eta})\phi_S\phi_T - 4rr_b\sqrt{(1-r^2)}\eta\phi_S^s\phi_T^s]\alpha_s(t_{g2})h_{g2}(\alpha_{g2}, \beta_{g2}, b_B, b_3) \exp[-S_B(t_{g2}) - S(t_{g2}) - S_3(t_{g2})] \\
& - [2r\sqrt{(1-r^2)}\eta(x_B - x_3\bar{\eta} - \eta)\phi_S^t(\phi_T^s - \bar{\eta}\phi_T^t) - r\sqrt{(1-r^2)}\eta(\bar{x}_B - z + x_3 + r^2(x_3 - \bar{z}) + \eta\bar{x}_3)(\phi_S^s - \phi_S^t)\phi_T^s \\
& + (r^2 - 1 - \eta)(r^2(\bar{x}_B - z\bar{\eta}) - \bar{\eta}\bar{z})\phi_S\phi_T - r\bar{\eta}\sqrt{(1-r^2)}\eta(\bar{x}_3\bar{\eta} + x_B - z + r^2(x_3 - \bar{z}))(\phi_S^s - \phi_S^t)\phi_T^t] \\
& \times \alpha_s(t_{h2})h_{h2}(\alpha_{h2}, \beta_{h2}, b_B, b_3) \exp[-S_B(t_{h2}) - S(t_{h2}) - S_3(t_{h2})] \}
\end{aligned} \tag{A.18}$$

$$\begin{aligned}
W_T^{LR} = & -\frac{32}{3}\pi C_F M_B^4 \int_0^1 dx_B dz dx_3 \int_0^\infty b_B db_B b_3 db_3 \phi_B(x_B, b_B) \\
& \times \{ [2r^2\sqrt{(1-r^2)}\eta(x_B - \bar{x}_3\bar{\eta} - r_b)\phi_S^t\phi_T + r((1-r^2)(\bar{x}_3 - x_B + r_b) + (z - \bar{x}_3 - r^2(z - 2\bar{x}_3) + r_b)\eta)\phi_S\phi_T^s \\
& + r\bar{\eta}(\bar{x}_3\bar{\eta} - x_B - z\eta + r^2(x_B - \bar{x}_3 + z\eta) - r_b(r^2 - \bar{\eta}))\phi_S\phi_T^t + \sqrt{(1-r^2)}\eta(z\bar{\eta} + r^2(x_B - z\bar{\eta}) - r_b(r^2 - \bar{\eta})) \\
& \times (\phi_S^s - \phi_S^t)\phi_T]\alpha_s(t_{g2})h_{g2}(\alpha_{g2}, \beta_{g2}, b_B, b_3) \exp[-S_B(t_{g2}) - S(t_{g2}) - S_3(t_{g2})] \\
& - [r\bar{\eta}((1-r^2)(x_B - z\eta) + x_3(r^2 - \bar{\eta}))\phi_S\phi_T^t - r((r^2-1)(x_B + (z-2)\eta) + x_3\bar{\eta} + (2\eta-1)r^2 x_3)\phi_S\phi_T^s \\
& - \sqrt{(1-r^2)}\eta(\bar{z}\bar{\eta} + r^2(z\bar{\eta} - \bar{x}_B))(\phi_S^s - \phi_S^t)\phi_T - 2r^2\sqrt{(1-r^2)}\eta(x_B - \eta - x_3\bar{\eta})\phi_S^t\phi_T] \\
& \times \alpha_s(t_{h2})h_{h2}(\alpha_{h2}, \beta_{h2}, b_B, b_3) \exp[-S_B(t_{h2}) - S(t_{h2}) - S_3(t_{h2})] \}
\end{aligned} \tag{A.19}$$

$$\begin{aligned}
W_T^{SP} = & \frac{32}{3}\pi C_F M_B^4 \int_0^1 dx_B dz dx_3 \int_0^\infty b_B db_B b_3 db_3 \phi_B(x_B, b_B) \\
& \times [(r_b(r^2 - \bar{\eta}) + (1-r^2 + \eta)(z\bar{\eta} + r^2(x_B - z\bar{\eta})))\phi_S\phi_T + 2r\sqrt{(1-r^2)}\eta(x_B - \bar{x}_3\bar{\eta})\phi_S^t(\phi_T^s - \bar{\eta}\phi_T^t) \\
& + r\sqrt{(1-r^2)}\eta(\phi_S^s - \phi_S^t)((x_B - z - \bar{x}_3\bar{\eta} + r^2(x_3 - \bar{z}))\phi_T^s + \bar{\eta}(\bar{x}_3\bar{\eta} - x_B - z + r^2(x_3 - \bar{z}))\phi_T^t) \\
& + 4rr_b\sqrt{(1-r^2)}\eta\phi_S^s\phi_T^s]\alpha_s(t_{g2})h_{g2}(\alpha_{g2}, \beta_{g2}, b_B, b_3) \exp[-S_B(t_{g2}) - S(t_{g2}) - S_3(t_{g2})] \\
& - [2r\sqrt{(1-r^2)}\eta(\bar{z} + r^2(x_3 - \bar{z}))\phi_S^t\phi_T^s + (r^2 - \bar{\eta})((r^2-1)(x_B + (z-2)\eta) + x_3\bar{\eta} + r^2 x_3(2\eta-1))\phi_S\phi_T \\
& + r\sqrt{(1-r^2)}\eta(\phi_S^s - \phi_S^t)((\bar{z} - x_B + x_3 + r^2(x_3 - \bar{z}) + \eta\bar{x}_3)\phi_T^s - \bar{\eta}(x_B - z + \bar{x}_3\bar{\eta} + r^2(x_3 - \bar{z}))\phi_T^t) \\
& - 2r\bar{\eta}\sqrt{(1-r^2)}\eta(\bar{z} + r^2(x_3 - \bar{z}))\phi_S^t\phi_T^t]\alpha_s(t_{h2})h_{h2}(\alpha_{h2}, \beta_{h2}, b_B, b_3) \exp[-S_B(t_{h2}) - S(t_{h2}) - S_3(t_{h2})]
\end{aligned} \tag{A.20}$$

The hard functions h_i are derived from the Fourier transform with $i = (a1, \dots, h2)$, whose specific expression is

$$\begin{aligned}
 h_i(\alpha, \beta, b_1, b_2) &= h_1(\alpha, b_1) \times h_2(\beta, b_1, b_2), \\
 h_1(\alpha, b_1) &= \begin{cases} K_0(\sqrt{\alpha}b_1), & \alpha > 0, \\ K_0(i\sqrt{-\alpha}b_1), & \alpha < 0, \end{cases} \\
 h_2(\beta, b_1, b_2) &= \begin{cases} \theta(b_1 - b_2)I_0(\sqrt{\beta}b_2)K_0(\sqrt{\beta}b_1) + (b_1 \leftrightarrow b_2), & \beta > 0, \\ \theta(b_1 - b_2)J_0(\sqrt{-\beta}b_2)K_0(i\sqrt{-\beta}b_1) + (b_1 \leftrightarrow b_2), & \beta < 0, \end{cases}
 \end{aligned} \tag{A.21}$$

with the Bessel function J_0 , and the modified Bessel functions K_0 and I_0 . The expressions for α and β in the hard functions are

$$\begin{aligned}
 \alpha_{(a1,b1)} &= \beta_{(c1,d1)} = M_B^2 r^2 x_3 (x_B - \bar{\eta} x_3), \\
 \beta_{a1} &= M_B^2 [(r^2 x_3 - 1)(1 - x_3 \bar{\eta}) + r_b^2], \\
 \beta_{b1} &= M_B^2 r^2 (x_B - \bar{\eta}), \\
 \alpha_{c1} &= M_B^2 [r^2 (z - \bar{x}_3) + \bar{z}] (x_B - \eta - x_3 \bar{\eta}), \\
 \alpha_{d1} &= M_B^2 [r^2 (x_3 - z) + z] (x_B - x_3 \bar{\eta}), \\
 \alpha_{(e1,f1)} &= \beta_{(g1,h1)} = M_B^2 \bar{x}_3 \bar{\eta} [r^2 (x_3 - \bar{z}) - z], \\
 \beta_{e1} &= M_B^2 (r^2 x_3 - 1)(1 - x_3 \bar{\eta}), \\
 \beta_{f1} &= M_B^2 \bar{\eta} (-r^2 \bar{z} - z), \\
 \alpha_{g1} &= M_B^2 \{ [r^2 (z - \bar{x}_3) + \bar{z}] (x_B - \eta - x_3 \bar{\eta}) + r_b^2 \}, \\
 \alpha_{h1} &= M_B^2 [r^2 (\bar{x}_3 - z) + z] (x_B - \bar{x}_3 \bar{\eta}), \\
 \beta_{(c2,d2)} &= M_B^2 (1 - r^2) x_B z, \\
 \alpha_{c2} &= M_B^2 [z - r^2 (z - \bar{x}_3)] (x_B - \bar{x}_3 \bar{\eta}), \\
 \alpha_{d2} &= M_B^2 [r^2 (x_3 - z) + z] (x_B - x_3 \bar{\eta}), \\
 \alpha_{(e2,f2)} &= \beta_{(g2,h2)} = M_B^2 [r^2 (z - \bar{x}_3) + \bar{z}] (-\eta - x_3 \bar{\eta}), \\
 \beta_{e2} &= M_B^2 [(1 - r^2) z - 1], \\
 \beta_{f2} &= M_B^2 (1 - r^2 \bar{x}_3) (-\eta - x_3 \bar{\eta}), \\
 \alpha_{g2} &= M_B^2 \{ [r^2 (\bar{x}_3 - z) + z] (x_B - \bar{x}_3 \bar{\eta}) + r_b^2 \}, \\
 \alpha_{h2} &= M_B^2 [r^2 (z - \bar{x}_3) + \bar{z}] (x_B - \eta - x_3 \bar{\eta}),
 \end{aligned} \tag{A.22}$$

The hard scales $t_i (i = a1, \dots, h2)$, which are taken to remove the large logarithmic radiative corrections, are given by

$$\begin{aligned}
 t_{a1} &= \text{Max} \left\{ \sqrt{|\beta_{a1}|}, 1/b_B, 1/b_3 \right\}, t_{b1} = \text{Max} \left\{ \sqrt{|\beta_{b1}|}, 1/b_B, 1/b_3 \right\}, \\
 t_{c1} &= \text{Max} \left\{ \sqrt{|\alpha_{c1}|}, \sqrt{|\beta_{c1}|}, 1/b_B, 1/b \right\}, t_{d1} = \text{Max} \left\{ \sqrt{|\alpha_{d1}|}, \sqrt{|\beta_{d1}|}, 1/b_B, 1/b \right\}, \\
 t_{e1} &= \text{Max} \left\{ \sqrt{|\beta_{e1}|}, 1/b, 1/b_3 \right\}, t_{f1} = \text{Max} \left\{ \sqrt{|\beta_{f1}|}, 1/b, 1/b_3 \right\}, \\
 t_{g1} &= \text{Max} \left\{ \sqrt{|\alpha_{g1}|}, \sqrt{|\beta_{g1}|}, 1/b_B, 1/b \right\}, t_{h1} = \text{Max} \left\{ \sqrt{|\alpha_{h1}|}, \sqrt{|\beta_{h1}|}, 1/b_B, 1/b \right\}, \\
 t_{c2} &= \text{Max} \left\{ \sqrt{|\alpha_{c2}|}, \sqrt{|\beta_{c2}|}, 1/b_B, 1/b_3 \right\}, t_{d2} = \text{Max} \left\{ \sqrt{|\alpha_{d2}|}, \sqrt{|\beta_{d2}|}, 1/b_B, 1/b_3 \right\}, \\
 t_{e2} &= \text{Max} \left\{ \sqrt{|\beta_{e2}|}, 1/b, 1/b_3 \right\}, t_{f2} = \text{Max} \left\{ \sqrt{|\beta_{f2}|}, 1/b, 1/b_3 \right\}, \\
 t_{g2} &= \text{Max} \left\{ \sqrt{|\alpha_{g2}|}, \sqrt{|\beta_{g2}|}, 1/b_B, 1/b_3 \right\}, t_{h2} = \text{Max} \left\{ \sqrt{|\alpha_{h2}|}, \sqrt{|\beta_{h2}|}, 1/b_B, 1/b_3 \right\}.
 \end{aligned} \tag{A.23}$$

The Sudakov exponents are defined as

$$\begin{aligned}
S_B &= s(x_B p_1^+, b_B) + \frac{5}{3} \int_{1/b_B}^t \frac{d\bar{\mu}}{\bar{\mu}} \gamma_q(\alpha_s(\bar{\mu})), \\
S &= s(z p^+, b) + s(\bar{z} p^+, b) + 2 \int_{1/b}^t \frac{d\bar{\mu}}{\bar{\mu}} \gamma_q(\alpha_s(\bar{\mu})), \\
S_3 &= s(x_3 p_3^-, b_3) + s(\bar{x}_3 p_3^-, b_3) + 2 \int_{1/b_3}^t \frac{d\bar{\mu}}{\bar{\mu}} \gamma_q(\alpha_s(\bar{\mu})),
\end{aligned} \tag{A.24}$$

with the anomalous dimension of the quark $\gamma_q = -\alpha_s/\pi$, and $s(Q, b)$ is the Sudakov factor, which can be found in Ref. [80]. Meanwhile, the threshold resummation factor $S_t(x)$ is taken from Ref. [81],

$$S_t(x) = \frac{2^{1+2c}\Gamma(\frac{3}{2}+c)}{\sqrt{\pi}\Gamma(1+c)} [x(1-x)]^c, \tag{A.25}$$

with the parameter $c = 0.3$.

-
- [1] D. C. Yan, Z. Rui, Y. Yan and Y. Li, Study of four-body decays $B_{(s)} \rightarrow (\pi\pi)(\pi\pi)$ in the perturbative QCD approach, *Eur. Phys. J. C* **83**, 974 (2023).
 - [2] Z. T. Zou, X. Yu and C. D. Lu, Nonleptonic two-body charmless B decays involving a tensor meson in the perturbative QCD approach, *Phys. Rev. D* **86**, 094015 (2012).
 - [3] W. Wang, B to tensor meson form factors in the perturbative QCD approach, *Phys. Rev. D* **83**, 014008 (2011).
 - [4] R. L. Workman *et al.* (Particle Data Group), Review of particle physics, *Prog.Theor.Exp.Phys.* **2022**, 083C01 (2022).
 - [5] H. Y. Cheng and R. Shrock, Some results on vector and tensor meson mixing in a generalized QCD-like theory, *Phys. Rev. D* **84**, 094008 (2011).
 - [6] D. M. Li, H. Yu and Q. X. Shen, Properties of the tensor mesons $f_2(1270)$ and $f_2'(1525)$, *J. Phys. G* **27**, 807-814 (2001).
 - [7] Y. Li, A. J. Ma, Z. Rui, W. F. Wang and Z. J. Xiao, Quasi-two-body decays $B_{(s)} \rightarrow P f_2(1270) \rightarrow P\pi\pi$ in the perturbative QCD approach, *Phys. Rev. D* **98**, 056019 (2018).
 - [8] X. Liu, R. H. Li, Z. T. Zou and Z. J. Xiao, Nonleptonic charmless decays of $B_c \rightarrow TP, TV$ in the perturbative QCD approach, *Phys. Rev. D* **96**, 013005 (2017).
 - [9] Q. Qin, Z. T. Zou, X. Yu, H. n. Li and C. D. Lü, Perturbative QCD study of B_s decays to a pseudoscalar meson and a tensor meson, *Phys. Lett. B* **732**, 36 (2014).
 - [10] Q. X. Li, L. Yang, Z. T. Zou, Y. Li and X. Liu, Calculation of the $B \rightarrow K_{0,2}^*(1430) f_0(980)/\sigma$ decays in the perturbative QCD approach, *Eur. Phys. J. C* **79**, 960 (2019).
 - [11] J. Dai and X. Q. Yu, Study of $B_s^0 \rightarrow TT(a_2(1320), K_2^*(1430), f_2(1270), f_2'(1525))$ in the perturbative QCD approach, *Phys. Rev. D* **109**, 016024 (2024).
 - [12] Q. Chang, L. Yang, Z. T. Zou and Y. Li, Study of the $B^+ \rightarrow \pi^+ (\pi^+\pi^-)$ decay in PQCD approach, *Eur. Phys. J. C* **84**, 753 (2024).
 - [13] W. S. Fang, Z. T. Zou and Y. Li, Phenomenological analysis of the quasi-two-body $B \rightarrow D(R \rightarrow) K\pi$ decays in PQCD approach, *Phys. Rev. D* **108**, 113007 (2023).
 - [14] W. Liu and X. Q. Yu, Contributions of S , P , and D - wave resonances to the quasi-two-body decays $B_s^0 \rightarrow \psi(3686, 3770) K\pi$ in the perturbative QCD approach, *Eur. Phys. J. C* **82**, 441 (2022).
 - [15] Y. Li, D. C. Yan, Z. Rui, L. Liu, Y. T. Zhang and Z. J. Xiao, Resonant contributions to three-body $B_{(s)} \rightarrow [D^{(*)}, \bar{D}^{(*)}] K^+ K^-$ decays in the perturbative QCD approach, *Phys. Rev. D* **102**, 056017 (2020).
 - [16] Y. Li, D. C. Yan, Z. Rui and Z. J. Xiao, S , P and D -wave resonance contributions to $B_{(s)} \rightarrow \eta_c(1S, 2S) K\pi$ decays in the perturbative QCD approach, *Phys. Rev. D* **101**, 016015 (2020).
 - [17] H. Y. Cheng, C. K. Chua, and K. C. Yang, Charmless hadronic B decays involving scalar mesons: Implications on the nature of light scalar mesons, *Phys. Rev. D* **73**, 014017 (2006).
 - [18] J. L. Ren, M. Q. Li, X. Liu, Z. T. Zou, Y. Li and Z. J. Xiao, The $B^0 \rightarrow J/\psi f_0(1370, 1500, 1710)$ decays: An opportunity for scalar glueball hunting, *Eur. Phys. J. C* **84**, 358 (2024).
 - [19] E. M. Aitala *et al.* (Fermilab E791 Collaboration), Study of the $D_s^+ \rightarrow \pi^- \pi^+ \pi^+$ decay and measurement of f_0 masses and widths, *Phys. Rev. Lett* **86**, 765 (2001).
 - [20] A. Gokalp, Y. Sarac and O. Yilmaz, An analysis of $f_0 - \sigma$ mixing in light cone QCD sum rules, *Phys. Lett. B* **609**, 291 (2005).
 - [21] N. N. Achasov, On the nature of the scalar $a_0(980)$ and $f_0(980)$ mesons, *Phys. At. Nucl.* **65**, 546 (2002).
 - [22] H. Y. Cheng, Hadronic D decays involving scalar mesons, *Phys. Rev. D* **67**, 034024 (2003).
 - [23] D. Barberis *et al.* (WA102 Collaboration), A coupled channel analysis of the centrally produced $K^+ K^-$ and $\pi^+ \pi^-$ final states in pp interactions at 450-GeV/c, *Phys. Lett. B* **462**, 462 (1999).
 - [24] X. G. He, G. N. Li and D. Xu, SU(3) and isospin breaking effects on $B \rightarrow PPP$ amplitudes, *Phys. Rev. D* **91**, 014029 (2015).

- [25] S. Kränkl, T. Mannel and J. Virto, Three-body non-leptonic B decays and QCD factorization, Nucl. Phys. B **899**, 247 (2015).
- [26] H. Y. Cheng, C. K. Chua and A. Soni, Charmless three-body decays of B mesons, Phys. Rev. D **76**, 094006 (2007).
- [27] H. Y. Cheng, C. K. Chua and Z. Q. Zhang, Direct CP violation in charmless three-body decays of B mesons, Phys. Rev. D **94**, 094015 (2016).
- [28] Y. Li, Comprehensive study of $\bar{B}^0 \rightarrow K^0(\bar{K}^0)K^\mp\pi^\pm$ decays in the factorization approach, Phys. Rev. D **89**, 094007 (2014).
- [29] W. F. Wang and H. n. Li, Quasi-two-body decays $B \rightarrow K\rho \rightarrow K\pi\pi$ in perturbative QCD approach, Phys. Lett. B **763**, 29 (2016).
- [30] Y. Li, A. J. Ma, W. F. Wang and Z. J. Xiao, Quasi-two-body decays $B_{(s)} \rightarrow P\rho \rightarrow P\pi\pi$ in perturbative QCD approach, Phys. Rev. D **95**, 056008 (2017).
- [31] Z. T. Zou, L. Yang, Y. Li and X. Liu, Study of quasi-two-body $B_{(s)} \rightarrow \phi(f_0(980)/f_2(1270) \rightarrow \pi\pi)$ decays in perturbative QCD approach, Eur. Phys. J. C **81**, 91 (2021).
- [32] Y. Li, W. F. Wang, A. J. Ma and Z. J. Xiao, Quasi-two-body decays $B_{(s)} \rightarrow K^*(892)h \rightarrow K\pi h$ in perturbative QCD approach, Eur. Phys. J. C **79**, 37 (2019).
- [33] D. C. Yan, Y. Yan and Z. Rui, CP-violating observables of four-body $B_{(s)} \rightarrow (\pi\pi)(K\bar{K})$ decays in perturbative QCD, Eur. Phys. J. C **84**, 754 (2024).
- [34] Y. Li, D. C. Yan, Z. Rui and Z. J. Xiao, Study of $B_{(s)} \rightarrow (\pi\pi)(K\pi)$ decays in the perturbative QCD approach, Eur. Phys. J. C **81**, 806 (2021).
- [35] Z. Rui, Y. Li and H. n. Li, Four-body decays $B_{(s)} \rightarrow (K\pi)_{S/P}(K\pi)_{S/P}$ in the perturbative QCD approach, J. High Energy Phys. **05** (2021) 082.
- [36] H. Q. Liang and X. Q. Yu, Study of the four-body decays $B_s^0 \rightarrow \pi\pi\pi\pi$ in the perturbative QCD approach, Phys. Rev. D **105**, 096018 (2022).
- [37] Z. R. Liang and X. Q. Yu, Perturbative QCD predictions for the decay $B_s^0 \rightarrow SS(a_0(980), f_0(980), f_0(500))$, Phys. Rev. D **102**, 116007 (2020).
- [38] M. Diehl, T. Gousset, and B. Pire, Exclusive production of pion pairs in $\gamma^*\gamma$ collisions at large Q^2 , Phys. Rev. D **62**, 073014 (2000).
- [39] C. H. Chen and H. n. Li, Vector-pseudoscalar two-meson distribution amplitudes in three-body B meson decays, Phys. Rev. D **70**, 054006 (2004).
- [40] C. H. Chen and H. n. Li, Three-body nonleptonic B decays in perturbative QCD, Phys. Lett. B **561**, 258 (2003).
- [41] B. Aubert *et al.* (BABAR Collaboration), Search for B-meson decays to two-body final states with $a_0(980)$ mesons, Phys. Rev. D **70**, 111102 (2004).
- [42] B. Aubert *et al.* (BABAR Collaboration), Dalitz-plot analysis of the decays $B^\pm \rightarrow K^\pm\pi^\mp\pi^\pm$, Phys. Rev. D **72**, 072003 (2006).
- [43] A. Garmash *et al.* (Belle Collaboration), Evidence for large direct CP violation in $B^\pm \rightarrow \rho(770)^0 K^\pm$ from analysis of three-body charmless $B^\pm \rightarrow K^\pm\pi^\pm\pi^\pm$ decays, Phys. Rev. Lett. **96**, 251803 (2006).
- [44] R. Aaij *et al.* (LHCb Collaboration), First observation of $\bar{B}^0 \rightarrow J/\psi K^+ K^-$ and search for $\bar{B}^0 \rightarrow J/\psi\phi$ decays, Phys. Rev. D **88**, 072005 (2013).
- [45] A. Garmash *et al.* (Belle Collaboration), Study of three-body charmless B decays, Phys. Rev. D **65**, 092005 (2002).
- [46] R. Zhou, Y. Q. Li, and J. Zhang, Isovector scalar $a_0(980)$ and $a_0(1450)$ resonances in the $B \rightarrow \psi(K\bar{K}, \pi\eta)$ decays, Phys. Rev. D **99**, 093007 (2019).
- [47] J. Chai, S. Cheng, and A. J. Ma, Probing isovector scalar mesons in the charmless three-body B decays, Phys. Rev. D **105**, 033003 (2022).
- [48] A. J. Ma, Y. Li, W. F. Wang and Z. J. Xiao, S-wave resonance contributions to the $B_{(s)}^0 \rightarrow \eta_c(2S)\pi^+\pi^-$ in the perturbative QCD factorization approach, Chin. Phys. C **41**, 083105 (2017).
- [49] J. W. Zhang, B. Y. Cui, X. G. Wu, H. B. Fu and Y. H. Chen, Quasi-two-body decays $B \rightarrow Pf_0(500) \rightarrow P\pi^+\pi^-$ in the perturbative QCD approach, Phys. Rev. D **110**, 036015 (2024).
- [50] H. Yang and X. Q. Yu, Investigating B_s three-body decays of scalar mesons in perturbative QCD approach, Phys. Rev. D **107**, 013001 (2023).
- [51] W. F. Liu, Z. T. Zou, and Y. Li, Charmless Quasi-two-body B decays in perturbative QCD approach: Taking $B \rightarrow K(\mathcal{R} \rightarrow)K^+K^-$ as examples, Adv. High Energy Phys. 5287693 (2022).
- [52] L. Yang, Z. T. Zou, Y. Li, X. Liu, and C. H. Li, Quasi-two-body $B_{(s)} \rightarrow V\pi\pi$ decays with resonance $f_0(980)$ in the PQCD approach, Phys. Rev. D **103**, 113005 (2021).
- [53] J. P. Lees *et al.* (BABAR Collaboration), B^0 meson decays to $\rho^0 K^{*0}$, $f_0 K^{*0}$, and $\rho^- K^{*+}$, including higher K^* resonances, Phys. Rev. D **85**, 072005 (2012).
- [54] G. Buchalla, A. J. Buras, and M. E. Lautenbacher, Weak decays beyond leading logarithms, Rev. Mod. Phys. **68**, 1125 (1996).
- [55] C. D. Lü, K. Ukai, and M. Z. Yang, Branching ratio and CP violation of $B \rightarrow \pi\pi$ decays in the perturbative QCD approach, Phys. Rev. D **63**, 074009 (2001).
- [56] Y. Y. Keum, H. n. Li, and A. I. Sanda, Penguin enhancement and $B \rightarrow K\pi$ decays in perturbative QCD, Phys. Rev. D **63**, 054008 (2001).
- [57] H. n. Li, Y. L. Shen and Y. M. Wang, Resummation of rapidity logarithms in B meson wave functions, J. High Energy Phys. **08**, (2013) 008.
- [58] H. Y. Cheng, Y. Koike, K. C. Yang, Two-parton light-cone distribution amplitudes of tensor mesons, Phys. Rev. D **82**, 054019 (2010).
- [59] H. Y. Cheng and K. C. Yang, Charmless hadronic B decays into a tensor meson, Phys. Rev. D **83**, 034001 (2011).
- [60] X. Ye and Z. P. Xing, S-wave contributions to $\bar{B}_s^0 \rightarrow (D^0, \bar{D}^0)\pi^+\pi^-$ in the perturbative QCD framework, Chin. Phys. C **43**, 073103 (2019).
- [61] W. F. Wang, J. Chai and A. J. Ma, Contributions of $K_0^*(1430)$ and $K_0^*(1950)$ in the three-body decays $B \rightarrow K\pi h$, J. High Energy Phys. **03**, (2020) 162.
- [62] J. Back *et al.*, Laura ++: A Dalitz plot fitter, Comput. Phys. Commun. **231**, 198 (2018).

- [63] R. Aaij *et al.* (LHCb Collaboration), Analysis of the resonant components in $\bar{B}^0 \rightarrow J/\psi \pi^+ \pi^-$, Phys. Rev. D **87**, 052001 (2013).
- [64] R. Aaij *et al.* (LHCb Collaboration), Measurement of resonant and CP components in $\bar{B}_s^0 \rightarrow J/\psi \pi^+ \pi^-$ decays, Phys. Rev. D **89**, 092006 (2014).
- [65] R. Aaij *et al.* (LHCb Collaboration), Dalitz plot analysis of $B^0 \rightarrow \bar{D}^0 \pi^+ \pi^-$ decays, Phys. Rev. D **92**, 032002 (2015).
- [66] Y. Li, A. J. Ma, W. F. Wang and Z. J. Xiao, The S-wave resonance contributions to the three-body decays $B_{(s)}^0 \rightarrow \eta_c f_0(X) \rightarrow \eta_c \pi^+ \pi^-$ in perturbative QCD approach, Eur. Phys. J. C **76**, 675 (2016).
- [67] W. F. Wang, H. n. Li, W. Wang and C. D. Lü, S-wave resonance contributions to the $B_{(s)}^0 \rightarrow J/\psi \pi^+ \pi^-$ and $B_s \rightarrow \pi^+ \pi^- \mu^+ \mu^-$ decays, Phys. Rev. D **91**, 094024 (2015).
- [68] M. Bargiotti *et al.* (OBELIX Collaboration), Coupled channel analysis of $\pi^+ \pi^- \pi^0$, $K^+ K^- \pi^0$ and $K^\pm K_S^0 \pi^\mp$ from $\bar{p}p$ annihilation at rest in hydrogen targets at three densities, Eur. Phys. J. C **26**, 371 (2003).
- [69] A. Abele *et al.*, $\bar{p}p$ annihilation at rest into $K_L K^\pm \pi^\mp$, Phys. Rev. D **57**, 3860 (1998).
- [70] C. Amsler *et al.* (Crystal Barrel Collaboration), Observation of a new $I^G(J^{PC}) = 1^-(0^{++})$ resonance at 1450 MeV, Phys. Lett. B **333**, 277 (1994).
- [71] D. Barberis *et al.* (WA102 Collaboration), A measurement of the branching fractions of the $f_1(1285)$ and $f_1(1420)$ produced in central pp interactions at 450 GeV/c, Phys. Lett. B **440**, 225 (1998).
- [72] W. F. Wang, L. F. Yang, A. J. Ma and A. Ramos, Low-mass enhancement of kaon pairs in $B^+ \rightarrow \bar{D}^{(*)0} K^+ \bar{K}^0$ and $B^0 \rightarrow D^{(*)-} K^+ \bar{K}^0$ decays, Phys. Rev. D **109**, 116009 (2024).
- [73] H. D. Niu, G. D. Li, J. L. Ren and X. Liu, Perturbative QCD analysis of neutral B-meson decays into $\sigma\sigma$, σf_0 and $f_0 f_0$, Eur. Phys. J. C **82**, 177 (2022).
- [74] X. Liu, Z. T. Zou, Y. Li and Z. J. Xiao, Phenomenological studies on the $B_{d,s}^0 \rightarrow J/\psi f_0(500)[f_0(980)]$ decays, Phys. Rev. D **100**, 013006 (2019).
- [75] S. Cheng and S. L. Zhang, $D_s \rightarrow f_0(980)$ form factors and the $D_s^+ \rightarrow (f_0(980) \rightarrow [\pi\pi]_S^{I=0}) e^+ \nu_e$ decay from light-cone sum rules, Eur. Phys. J. C **84**, 379 (2024).
- [76] R. Fleischer, R. Knegjens, and G. Ricciardi, Anatomy of $B_{s,d}^0 \rightarrow J/\psi f_0(980)$, Eur. Phys. J. C **71**, 1832 (2011).
- [77] M. Ablikim *et al.* (BES Collaboration), Evidence for $f_0(980)f_0(980)$ production in χ_{c0} decays, Phys. Rev. D **70**, 092002 (2004).
- [78] M. Ablikim *et al.* (BES Collaboration), Partial wave analysis of $\chi_{c0} \rightarrow \pi^+ \pi^- K^+ K^-$, Phys. Rev. D **72**, 092002 (2005).
- [79] K. M. Ecklund *et al.* (CLEO Collaboration), Study of the semileptonic decay $D_s^+ \rightarrow f_0(980) e^+ \nu$ and implications for $B_s^0 \rightarrow J/\psi f_0$, Phys. Rev. D **80**, 052009 (2009).
- [80] H. n. Li and K. Ukai, Threshold resummation for nonleptonic B meson decays, Phys. Lett. B **555**, 197 (2003).
- [81] T. Kurimoto, H. n. Li, and A. I. Sanda, Leading-power contributions to $B \rightarrow \pi, \rho$ transition form factors, Phys. Rev. D **65**, 014007 (2001).